Chemical Engineering & Processing: Process Intensification 201 (2024) 109832

Contents lists available at ScienceDirect

Chemical Engineering and Processing - Process Intensification

journal homepage: www.elsevier.com/locate/cep

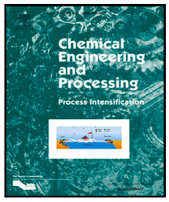

Optimal design and operation of reactive distillation systems and reactive dividing wall systems with pressure swing distillation and hybrid distillation-pervaporation

Fanyi Duanmu, Dian Ning Chia, Aikaterini Tsatse, Eva Sorensen *

Department of Chemical Engineering, University College London, Torrington Place, London WC1E 7JE, UK

ARTICLE INFO

Keywords:
Reactive distillation
Hybrid distillation
Dividing wall column
Pervaporation
Hybrid reactive dividing wall column

ABSTRACT

Process intensification is essential in exploring more energy-efficient processes, and key examples related to fluid separations are reactive distillation and hybrid distillation-pervaporation processes. This work will consider the reaction and separation of a general quaternary reactive system with a minimum boiling binary azeotrope AC, in a reactive distillation column where, given the thermodynamics limitations, further downstream separation is required. Low and high chemical equilibrium is considered for the reaction. For the downstream purification, both pressure swing distillation and a hybrid distillation-pervaporation process are considered. For each of the structures, their intensified equivalent dividing wall structures are also considered, including a hybrid reactive dividing wall system. It is shown that reactive distillation followed by a hybrid distillation-pervaporation system can save up to 24% energy compared to reactive distillation with pressure swing separation, and that the dividing wall column counterpart structures have lower production-based total annualised costs than the corresponding base systems.

1. Introduction

Process Intensification (PI) has received considerable attention over the past few decades as part of an effort to increase the efficiency and economic performance of chemical processes while minimising environmental impact. The main examples of PI related to separation processes are reactive distillation (RD), hybrid distillation processes, and dividing wall columns (DWCs). RD is a process that integrates a reactive process and a separation process into one process in a single column shell. The synergistic effects between the two processes significantly reduce energy requirements and thereby operating cost, and using a single column shell also greatly reduces capital cost [1,2]. Hybrid distillation integrates at least one distillation process with at least one other separation process [3], and one of the most popular examples is the hybrid with a membrane process, of which pervaporation is a more commonly used membrane type. A hybrid distillation-pervaporation (DP) process is particularly beneficial when separating azeotropic or close-boiling mixtures by exploiting the separation mechanism of the membranes which does not rely on vapour–liquid equilibrium. DP processes have been claimed to save energy compared to their conventional counterparts, such as extractive distillation and azeotropic distillation [4–6].

For multi-component systems, i.e., ternary and quaternary systems, where two or more distillation columns are normally required for the separation, the distillation columns can be integrated into a single column shell in a dividing wall column. DWCs can offer significant energy savings due to the thermal coupling streams, as well as significant capital cost savings as only one column shell is required [7,8]. Our team has performed extensive studies on the optimal design and operation of RD processes [9–11], DP processes [12,13], and DWC systems [14,15]. We recently integrated the DP and DWC processes into a hybrid dividing wall column (HDWC) and demonstrated that the HDWC design has great economic potential [12]. This work will incorporate reactive distillation and a hybrid dividing wall column into an even more intensified process to form a **hybrid reactive dividing wall column (HRDWC)**.

Few studies have considered HRDWC. Holtbruegge et al. [16] designed an HRDWC with a vapour permeation membrane for a transesterification process and compared the HRDWC with other possible configurations on a cost basis, including a system of a reactor followed by pressure swing (PS) designs (in the following referred to as the base case), RD with pressure swing distillation (RD-PS), reactive dividing wall column with pressure swing distillation (RDWC-PS), and RD with vapour permeation. The comparison showed that applications

* Corresponding author.
E-mail address: e.sorensen@ucl.ac.uk (E. Sorensen).

https://doi.org/10.1016/j.cep.2024.109832
Received 30 January 2024; Received in revised form 24 April 2024; Accepted 23 May 2024
Available online 24 May 2024

Nomenclature

Symbols

RR_n	Reflux ratio of column Cn (mol mol^{-1})
B_n	Bottoms flow rate of column Cn (kmol j^{-1})
D_n	Distillate flow rate of column Cn (kmol j^{-1})
$F_{\mathrm{tc}n,\mathrm{botV}}$	Flow rate of the bottom vapour thermal coupling stream of column Cn (kmol j^{-1})
$F_{\mathrm{tc}n,\mathrm{topL}}$	Flow rate of the top liquid thermal coupling stream of column Cn (kmol j^{-1})
N_{ms}	Number of membrane stages in the membrane network (–)
$N_{\mathrm{rxn,start/end}}$	Start/End stages of the reactive zone in the reactive distillation column (–)
$N_{\mathrm{mm},n}$	Number of membrane modules in membrane stage n (–)
$N_{\mathrm{sl}n,k}$	kth liquid side draw location of column Cn (–)
$N_{\mathrm{tc}n,\mathrm{botL/V}}$	Bottom liquid/vapour thermal coupling stream of column Cn (–)
$N_{\mathrm{tc}n,\mathrm{topL/V}}$	Top liquid/vapour thermal coupling stream of column Cn (–)
$N_{fn,k}$	kth feed stage of column Cn (–)
N_{tn}	Total number of stages of column Cn (–)
P_{pump}	Outlet pressure of the pump (atm)
P_n	Operating pressure of column Cn (atm)

Abbreviations

-Bot	(H)DWC structures with the dividing wall extended to the bottom
-Mid	(H)DWC structures with the dividing wall in the middle
CAPEX	Capital cost/expenditure
DP	Hybrid distillation-pervaporation
GA	Genetic Algorithm
HDWC	Hybrid dividing wall column
HRDWC	Hybrid reactive dividing wall column
MINLP	Mixed Integer Non-linear Programming
OPEX	Operating cost/expenditure
PI	Process Intensification
PS	Pressure swing
PSO	Particle Swarm Optimisation
RD	Reactive distillation
RDWC	Reactive dividing wall column
TAC	Total annualised cost

with membrane units and/or RDWC could significantly reduce operating costs, and the best design with the lowest total annualised cost (TAC) was RDWC-PS, followed by HRDWC. Wang et al. [17] compared HRDWC using a pervaporation membrane system to RD and RDWC as well as to three configurations of RD with a pervaporation membrane using a case study of isopentyl acetate production from mixed PVA by-products. The results showed that HRDWC had the lowest TAC (e.g., 35.6% TAC saving compared with RD) and was the second-best design for CO_2 emission, which indicated the great economic and environmental benefits of HRDWC for this system. Although both studies showed that HRDWC was economically superior to their conventional counterparts, the studies were limited to specific systems, conditions, and designs, which may not reflect the general performance of HRDWC.

Therefore, in this work, a fundamental study of the effects of chemical equilibrium on the separation and economic performance of the hybrid reactive process (e.g., RD-DP and HRDWC) will be compared with conventional reactive processes. The chemical equilibrium directly affects the conversion of reactants. Also, in terms of potential azeotropes, we will consider e.g., a binary azeotrope that is formed between a reactant and a product, and where the composition of the mixture may be located on different sides of the azeotropic point for different chemical equilibrium (e.g., high chemical equilibrium may mean that more reactant is consumed, thus less azeotrope is formed, so the composition of the mixture is different compared to the case of low chemical equilibrium). In this work, a reversible reaction (A + B ⇌ C + D), where one of the reactants (A) forms a minimum boiling azeotrope with one of the products (C), will be considered. An example of such a system is the transesterification of glycerol and dimethyl carbonate, where a minimum boiling azeotrope is formed between the reactant (dimethyl carbonate) and the by-product (methanol) [18–20]. The framework on how to design HRDWCs will be proposed. A study of the effects of chemical equilibrium on HRDWC designs via detailed optimisation and techno-economic analysis is essential to understanding and promoting the development of such highly integrated designs.

In the following, we will first set out the methodology we have followed for our investigation (Section 2), and then introduce the chemical systems, potential reactive structures, as well as the optimisation methods applied for this work. Next, the case study section (Section 3) will discuss the details (e.g., process parameters) of the mixtures and the chemical systems applied. Lastly, the optimisation results and a comparison between different structures (e.g., RD-PS, HRDWC, and their corresponding dividing wall modifications) under low and high chemical equilibrium are performed in Section 4. The results will show that the hybrid process can save significant energy, and that a reactive dividing wall structure can lead to lower production-based total annualised cost.

2. Methodology

In this section, the complexity of RD will be briefly discussed. Based on the aim of this work, a quaternary mixture with a binary azeotrope formed between one of the reactants and one of the products is considered, and for both low and high chemical equilibrium. Furthermore, two distillation sequences based on either pressure swing or a pervaporation membrane system are developed and considered along with their corresponding process intensification alternatives (i.e., a dividing wall structure). Finally, the details of the model and optimisation methods are briefly discussed.

2.1. Selected reaction system

This work considers a reversible unity stoichiometry reaction system involving two reactants and two products:

$$A + B \rightleftharpoons C + D \tag{1}$$

This type of reaction has been used in theoretical studies [9] and is also seen in industrial reaction systems (e.g., transesterification of glycerol and dimethyl carbonate) [18–20]. Other assumptions made are:

- Only one homogeneous minimum boiling azeotrope is present, and is formed between the lighter reactant A and product C (i.e., the azeotrope is AC)
- The azeotrope is pressure sensitive (shown in Fig. 1)
- The boiling point order (low to high) is: AC < C < A < D < B
- A heterogeneous catalytic reaction is considered
- For the pervaporation system, component A permeates through the membrane whilst the other components are retained

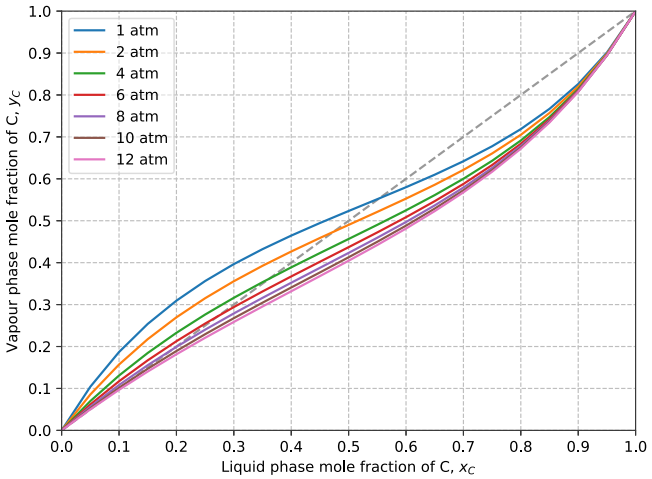

Fig. 1. The x–y diagram for components A and C at different pressures with component C (i.e., lighter component) as the basis showing the shift of azeotropic point to the left as pressure increases obtained using UNIQUAC as the thermodynamic model. The intersections between the curves and the diagonal line are the azeotropic points for the azeotrope AC.

The effects of the chemical equilibrium (i.e., low or high reaction conversion; details in Section 3) on the optimal designs will also be studied. The relevant structures for handling this reaction system are discussed in Section 2.2. Although our discussion will be limited to the system outline above, the general methodology for optimisation and analysis of reactive systems can obviously be employed also for other systems. Moreover, starting from a relatively simple reactive azeotropic system as described above allows one, in this proof-of-concept stage, to observe and analyse the underlying basic interactions/phenomena that would potentially be masked if a more complex system was used. Further discussions regarding the modifications to the structure that may be required for other separation mixtures can be found in Section 4.4.

The RD applications are more common for exothermic reactions. One typical advantage for exothermic reactions but not for endothermic reactions is that the energy released from the exothermic reaction can be used in the column to reduce energy consumption [21]. Other than that, many theoretical studies focus on exothermic reactions, so it should be noted that some design decisions may not be the same for endothermic reactions. However, this consideration would mainly affect the energy required but will not greatly impact the structure/design (e.g., in [22], the structure of the RD column did not change, but the reboiler duty increases when the reaction changes from highly exothermic to highly endothermic). Therefore, this work will not study the effect of the type of reactions.

2.2. Designs

There are various process unit arrangements for handling a system consisting of a reaction and one or more separations, and the conventional method is to use a reactor of some form followed by the separation, typically a distillation column. The interest in PI has boosted the research and development of RD columns, which integrate the reaction into the distillation column, thus reducing the number of units. The benefits of RD, such as increased conversion and selectivity, reduced energy consumption, and capital saving, have been discussed by many [23–25] so will not be repeated here. In this work, only processes that involve RD columns are considered (i.e., the conventional process is not discussed). Since in our case the azeotrope is assumed to be formed between one product and one reactant, the reaction is reversible, and the heaviest component is a reactant, additional units are required to address the separation of the azeotrope and to recycle any unreacted reactants. Common separation processes for dealing with azeotropes include extractive distillation, azeotropic distillation, pressure swing distillation, and membrane systems (e.g., DP process). Extractive and azeotropic distillation processes require an entrainer specific to the given mixture. As this work considers a reaction for artificial components (see Section 3 for more details), extractive and azeotropic distillation processes are not investigated. We have assumed that the azeotrope is pressure-sensitive. Therefore, PS distillation as well as DP processes are considered in conjunction with the RD column. The corresponding reactive dividing wall structures are also developed for comparison, and all configurations are shown in Fig. 2 (with the detailed membrane network shown in Fig. 3), with the simulation structures shown in Fig. 4 and discussed in the following.

2.2.1. General design concepts

The thought process when generating the processes shown in this work will be discussed before delving into the details of each design. First of all, the feeds to the first column are the reactants A and B, so column C1 must have a reactive section (i.e., column C1 is an RD column). Then, products C and D will be generated from the reactive section. Once product C is generated, for the reactive system considered in this work, it will form a minimum boiling azeotrope with any unreacted reactant A. Therefore, other than allowing reactions to occur, column C1 is also responsible for simultaneously separating as much azeotrope AC as possible from the mixture.

The bottom stream of column C1 contains mainly the unreacted reactants and the by-product D, so the purpose of column C2 (where the feed to column C2 is the bottom stream of column C1) is to recover the unreacted reactants and recycle them back into column C1. Since the majority of distillate from column C1 is the azeotrope AC containing unreacted reactant A and valuable product C, a separation technique is required to recover reactant A and to obtain pure product C. The presence of an azeotrope and the need for separating it means that a single distillation column is insufficient. Any separation technique capable of handling azeotropes can be considered, and in this work, both PS distillation (recall that the azeotrope is pressure-sensitive) and pervaporation membrane are considered.

With the concepts above, the basic structures (e.g., Fig. 2(a)) can be generated. Then, by analysing the compositions of the outlet streams from the distillation columns, streams with similar compositions may be coupled as thermal coupling streams. As the thermal coupling streams should be the ends of the wall section in a DWC, by identifying the thermal coupling streams, the corresponding DWC structures can also be generated (e.g., transformation of Fig. 2(a) into Figs. 2(b) and 2(c); more details in the following sections).

2.2.2. Reactive distillation-pressure swing (RD-PS) structures

The configuration for the RD-PS option is shown in Fig. 2(a). It should be noted that the PS system can only be used for pressure-sensitive azeotropic systems, as assumed in this work. The reactants, A and B, are fed into the reactive column C1, where the feed location of the higher boiling component B is located above the feed location of the lower boiling component A. Also, since the reaction is assumed to be heterogeneously catalytic, the start and end stages can be optimised and the reaction will be confined to between these stages. A discussion of the effect of the feed locations of A and B, as well as the effect of the start and end stages of the reactive stages, can be found in Section S1 in the supplementary material. In column C1, the top stream mainly contains the minimum-boiling azeotrope AC while the bottom stream mainly contains components B and D. It should be noted that if the start of the reactive zone is close to the top of column C1, the distillate may also contain components B and D, thus the bottom stream from column C2 may also contain B and D. A similar case may also be possible for the bottom stream in column C1 (i.e., may also contain traces of components A and C). For the bottom stream from column C1, since components B and D do not form an azeotrope, a conventional distillation column (C2) is enough to perform the separation. A nearly

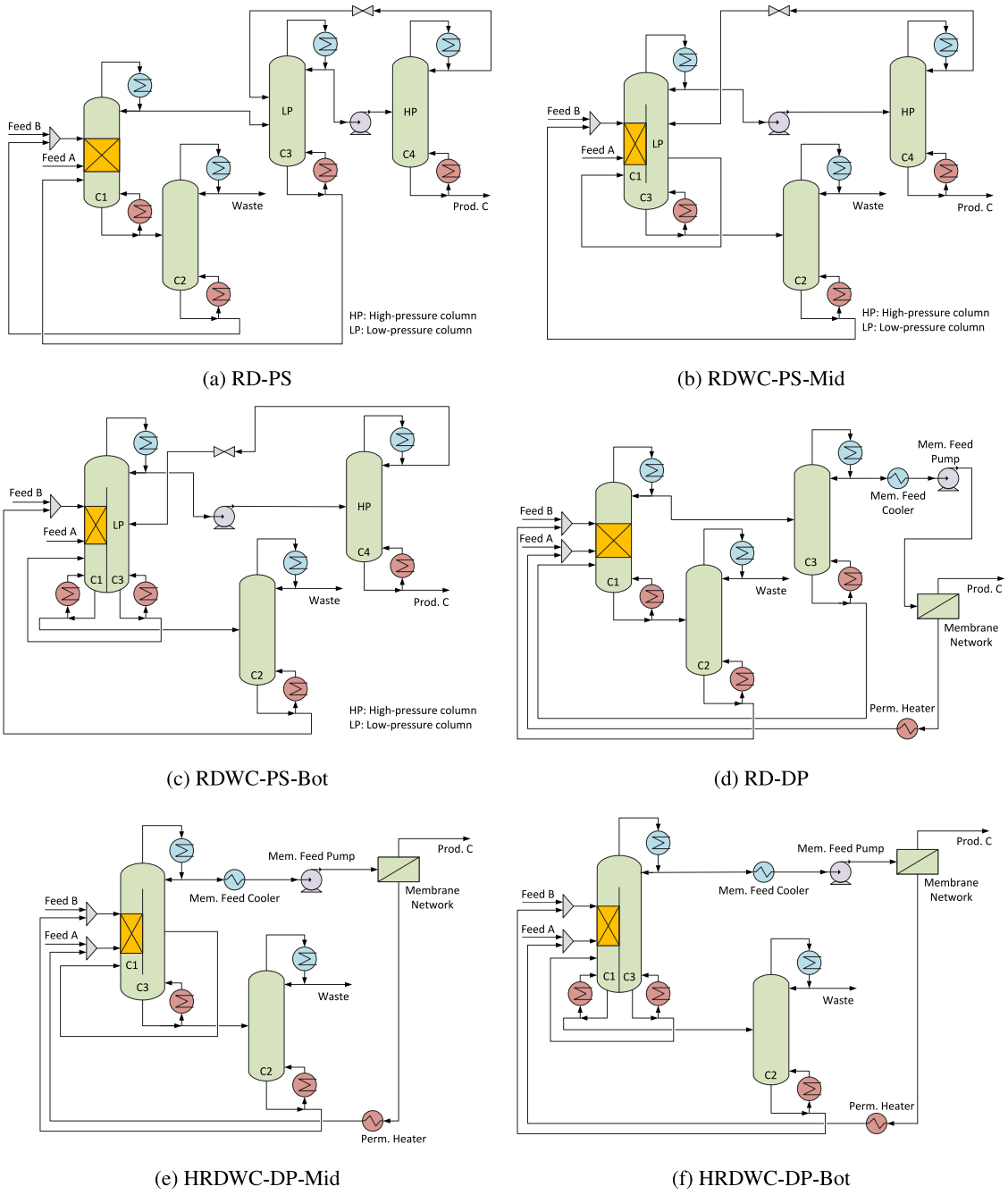

Fig. 2. Low chemical equilibrium — Flowsheets of the reactive distillation (RD) and its reactive dividing wall column (RDWC) or hybrid reactive dividing wall column (HRDWC) counterparts with (a,b,c) pressure swing (PS) and (d,e,f) distillation-pervaporation (DP), where (b,e) have the dividing wall in the middle of the column (-Mid) and (c,f) have the dividing wall extended to the bottom of the column (-Bot). The detailed membrane network is shown in Fig. 3.

pure reactant B is recovered in the bottom stream of column C2, and is mixed with fresh component B before being recycled back into column C1. The distillate of column C1 enters a PS process to separate the azeotrope AC. Depending on the azeotropic composition of the feed stream into column C3 (i.e., located on either side of the azeotropic point), the column pressure (high-pressure column or low-pressure column) and the main component in the bottom stream vary. For a case where the azeotropic point is on the left-hand side in Fig. 1, column C3 operates at a lower pressure (e.g., atmospheric pressure), and its main task is to separate the azeotrope from the mixture (recall that azeotrope AC is minimum boiling) in the distillate. In this work, the lowest operating pressure considered for a distillation column is atmospheric pressure. The bottom of column C3, mainly component A, is recycled back into column C1, although separately without mixing with feed stream A. This is to reduce the mixing effect, thus a waste of energy, because the bottom stream from column C3 may contain some component D and therefore the stream composition may be different from the pure feed stream A. Although in the figure (Fig. 2(a)), the feed stage of the recycled stream is below the feed location of pure A, for the optimal design in this work, the feed stage of the recycled stream is optimised freely, similarly for all other feed/sidedraw locations in any units and any structures. The distillate from column C3 will be pressurised in a pump before entering the next column C4 (higher pressure column). As the vapour–liquid equilibrium of a binary mixture differs under different pressures, the azeotrope composition shifts with the pressure. Therefore, by changing the pressure in the second column (C4), the azeotrope will shift from one side of the azeotropic point to the other side, so the separation can continue to purify another

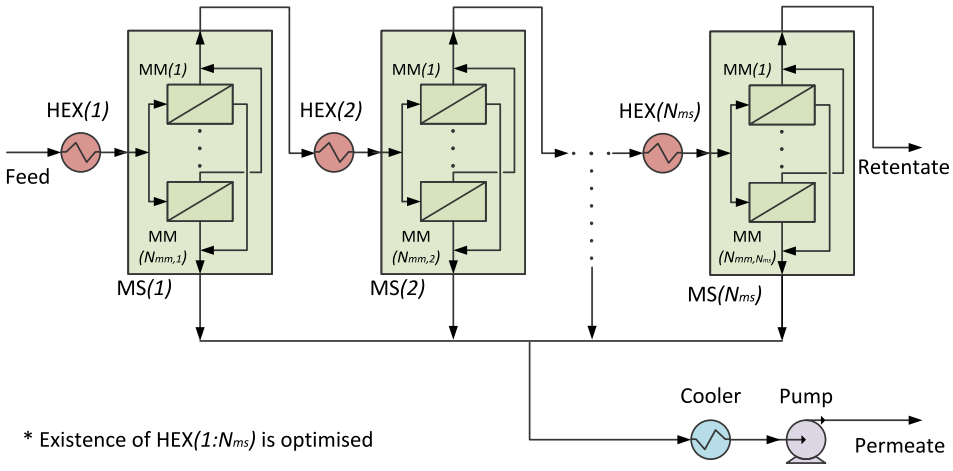

Fig. 3. Schematic of the membrane network, where the membrane stages (MS) are the larger boxes and the membrane modules (MM) are the smaller boxes with a diagonal line, HEX(n) is the nth membrane stage feed heater, N_{ms} is the number of membrane stages in a membrane network, and $N_{mm,n}$ is the number of membrane modules in the nth membrane stage.
Source: Taken from [12].

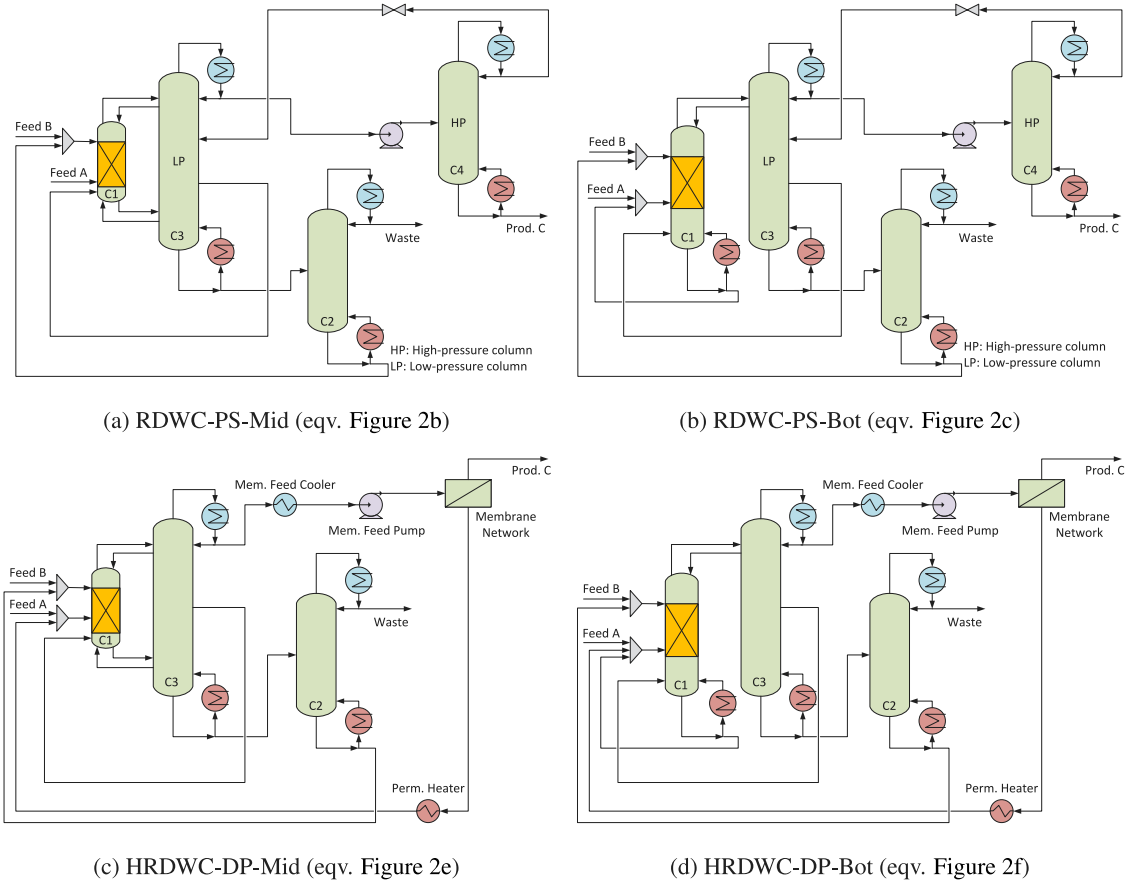

(a) RDWC-PS-Mid (eqv. Figure 2b)

(b) RDWC-PS-Bot (eqv. Figure 2c)

(c) HRDWC-DP-Mid (eqv. Figure 2e)

(d) HRDWC-DP-Bot (eqv. Figure 2f)

Fig. 4. Low chemical equilibrium — The Petlyuk structures used in simulations for the reactive dividing wall column (RDWC) with pressure swing (PS) where the wall is (a) located in the middle (RDWC-PS-Mid) or (b) extended to the bottom (RDWC-PS-Bot), and hybrid reactive dividing wall column (HRDWC) with distillation-pervaporation (DP) where the wall is located in the middle (HRDWC-DP-Mid) or (d) extended to the bottom (HRDWC-DP-Bot).

component (e.g., component C in this work) and the minimum boiling azeotrope can be recycled back to the previous column (C3).

Further process intensification can be applied to the RD-PS structure to form a reactive dividing wall column followed by a pressure swing structure (RDWC-PS). In this work, two different RDWC-PS structures are explored, where the wall is: (1) located in the middle of the main column, as normally seen in a DWC, and (2) extended to the bottom of the main column. The RDWC-PS structures with the wall located in the middle and the wall extended to the bottom are denoted as RDWC-PS-Mid (Fig. 2(b)) and RDWC-PS-Bot (Fig. 2(c)), respectively. The descriptions for these structures can be found in the next paragraph. In both of the RDWC variations of the RD-PS structure, the pressures at the ends of the dividing wall would need to be the same. This can be achieved by using the same number of trays with identical properties

(i.e., same pressure drop per stage) on both sides of the wall or using a different number of trays with different pressure drop properties while maintaining the overall pressure drop from the top to the end of the wall the same on both sides. For either condition, this constraint should be considered during design and optimisation. Further discussion can be found in Section 2.3.

Both the RDWC-PS variations integrate columns C1 and C3 into a single column shell to form the RDWC, with the location of the wall as the only difference. The distillates of columns C1 and C3 contain mainly the azeotrope, so they can "share" the same top stages and distillate in the RDWC. However, the compositions of the bottom streams of columns C1 and C2 are different (recall that as the azeotropic point is on the left-hand side in Fig. 1, the bottom of column C1 contains mainly components B and D while the bottom of column C3 contains components A and potentially some D), so the bottom streams of columns C1 and C3 should not be "combined". This then leads to the two different locations of the wall — RDWC-PS-Mid (Fig. 2(b)) and RDWC-PS-Bot (Fig. 2(c)). The formation of RDWC-PS-Mid is based on the designs of conventional DWCs where the wall is located in the middle so that the middle boiling components (in this case, components A and D; recall that the boiling point in increasing order for the system considered is AC < C < A < D < B) can be freely distributed between the top and bottom of the wall. Then, in RDWC-PS-Mid, a side stream which contains mainly components A and D is extracted from the main column side (i.e., column C3) and sent back to the prefractionator column side (i.e., column C1). The bottom stream from the RDWC is sent to column C2 for further separation as before. For RDWC-PS-Bot, since the bottom stream compositions of columns C1 and C3 are different, they do not have to "share" the same stages at the bottom, so the wall can extend all the way to the bottom of the main column. Then, the bottom stream of the main column (i.e., column C3) is recycled back to column C1, and the bottom stream of the prefractionator column (i.e., column C1) is sent to column C2 for further separation.

2.2.3. Hybrid distillation-pervaporation (DP) processes

A DP process consists of at least one distillation column and one membrane unit, the latter commonly considered to be a pervaporation unit. The flowsheets of the reactive distillation-DP (RD-DP) and its hybrid reactive dividing wall column (HRDWC-DP) variations are shown in Figs. 2(d)–2(f). In a pervaporation membrane system, the feed and retentate streams are in the liquid phase, while the permeate stream is in the vapour phase. The phases of the streams are typically ensured by operating the feed and retentate side of the membrane at a high pressure and the permeate side of the membrane at a low pressure (commonly at a vacuum). The purpose of the membrane is to break the azeotrope, where one of the components from the azeotrope should be separated from the other components by crossing the membrane. In this work, the membrane separates the azeotrope AC by allowing component A to permeate through the membrane, so component A will be collected in the permeate while component C will be collected in the retentate. For better visualisation of the flowsheets in Fig. 2, the membrane network is shown simply with a rectangular box with a diagonal line instead of drawing the whole membrane network. The detailed membrane network can be found in Fig. 3, based on the concept introduced by Marriott and Sorensen [26]. There are two important concepts in the membrane network, which are the (1) membrane *module* that is a typical membrane unit, and (2) membrane *stage* that is a collection of membrane modules connected in parallel. In a membrane network, N_{ms} membrane stages are connected in series, while in a membrane stage n, $N_{\mathrm{mm},n}$ membrane modules are connected in parallel. The number of membranes per stage does not have to be the same. HEX(n) is the feed heater for membrane stage n, and the existence of each feed heater is a degree of freedom that is optimised. The retentate from membrane stage $n-1$ is the feed of membrane stage n, and the permeate streams from each membrane stage are combined into a final permeate stream. The final permeate stream (recall that it is in a vapour phase) then enters a cooler to be cooled down into a liquid and passed through a pump to raise its pressure to the atmospheric or operating pressure of the subsequent unit, but note that this will bring the permeate stream into a sub-cooled phase. Therefore, as seen in Figs. 2(d)–2(f), a permeate heater is used to bring the sub-cooled permeate back into a saturated liquid phase. However, this step is not compulsory because the flow rate of the permeate stream is generally low, so directly feeding the sub-cooled permeate into the distillation column may not disrupt the vapour–liquid equilibrium in the distillation column by much. If the permeate heater is not used, the energy required to heat the sub-cooled permeate stream will be transferred to the reboiler of the distillation column, so the overall performance (total annualised cost) will not be greatly affected. Note that other membrane network arrangements can also be used.

Fig. 2(d) shows the flowsheet of RD-DP, and the working principles of the RD column C1 and conventional distillation column C2 are the same as mentioned in Section 2.2.2. The feed into conventional distillation column C3 contains mainly components A and C, and the purpose of column C3 is to separate the azeotrope AC from the mixture in the distillate so that the pervaporation membrane that is located there can further separate the azeotrope AC into pure components A and C. The permeate contains almost pure unreacted component A, so it is mixed with fresh component A feed before recycling back into column C1. The bottom of column C3 is recycled back into column C1 without mixing with any other streams, as discussed in Section 2.2.2 to avoid the mixing effect. Similarly to the process intensification discussed in Section 2.2.2, two HRDWC structures can be formed with the dividing wall located in the middle (HRDWC-DP-Mid, see Fig. 2(e)) and extended to the bottom (HRDWC-DP-Bot, see Fig. 2(f)).

2.3. Simulation and optimisation

All studies in this work are performed in gPROMS Process [27], and the built-in library models are used for simulating the standard and RD columns (considering equilibrium is established on each stage, i.e., equilibrium model), heaters, coolers, and pumps. Due to the lack of a library for DWCs, the corresponding thermodynamically equivalent Petlyuk designs shown in Fig. 4 are used instead.

For the pervaporation membrane model, a user-defined model is used. A detailed discussion of the methodology and mathematical models for the pervaporation membrane and the membrane network superstructure can be found in our previous work [13]. The pervaporation membrane model is a solution–diffusion model initially proposed by Tsuyumoto et al. [28], and the membrane network superstructure (shown in Fig. 3) originates from Marriott and Sorensen [26]. The membrane network superstructure allows the optimisation of the number of membrane stages in series and the number of membrane modules in each of the membrane stages. In this work, the same configuration and membrane parameters as in Chia et al. [12] are used. Note that since the components in this work are artificial, the membrane parameters are also artificial. Rather than completely making up the values for the membrane parameters, the parameters from Tsuyumoto et al. [28] are adopted by considering component A as the component permeating through the membrane. Discussions on the adaptation of the membrane parameters can be found in the appendix of Chia et al. [12]. The original membrane model proposed by Tsuyumoto et al. [28] only considers a binary mixture. In our work, the feed stream into the membrane is assumed to only contain two components (A and C) which is guaranteed by including an optimisation constraint where the composition of components B and D in the membrane feed stream should be less than a small value (e.g., $\leq 0.0001\ \mathrm{mol\,mol^{-1}}$). If other membrane models are used, where data is available for all components, this constraint will not be needed (but may still be useful for optimisation).

A step-wise flowsheet for the initialisation, simulation, and optimisation of hybrid processes introduced in our previous work [13] is

applied in this work. In brief, each unit (e.g., distillation column and membrane network) is first simulated individually using an approximated feed information. The simulation results of each unit will be saved and serve as preset (i.e., initial) values for the simulation of the complete design.

In terms of optimisation, the discrete variables (e.g., total number of stages, feed locations, reactive stages, and the number of membrane modules) together with continuous variables (e.g., reflux ratio, bottom flow rate, and pump pressure) make the optimisation a Mixed Integer Non-linear Programming (MINLP) problem. Two different stochastic optimisation methods, Genetic Algorithm (GA) and Particle Swarm Optimisation (PSO), are used in this work. The better optimal design from these two (solely based on the objective value) will be chosen for comparison with other structures. As GA and PSO are unavailable in gPROMS, we developed the optimisation algorithms in C# serving as black-box external optimisers and connected these with gPROMS via gO:Run [29]. For the implementation of GA in this work, the tournament selection with four individuals is used as the parent selection method [30]. Moreover, the flat crossover [31] and uniform mutation [30] are used to update individuals. For PSO, the inertia is dynamically chosen in each iteration using the random adjustments method, and the cognitive (resp. social) acceleration coefficient is linearly decreased (resp. increased) [32]. The random forth method [33] is used for the boundary handling. For both GA and PSO, the constraint handling method proposed by Deb [34] is applied to avoid defining the R value for the fitness penalty. According to the algorithm proposed by Deb [34], the objective function is written in a way that (1) if any constraints are violated, the solution is considered undesired, so the objective function is modified to the summation of the worst feasible solution and the degree of constraint violation, or (2) if none of the constraints are violated, the objective function value is unmodified. 100 chromosomes/swarms/individuals are used. The stopping criteria can be either (1) 200 maximum iterations reached, or (2) the best fitness stays constant for 20 consecutive iterations, depending on which criteria is achieved first. Other information, such as the optimisation variables, objective functions, and constraints, will be discussed with the selected case studies in Section 3.

3. Case studies

A general reaction A + B ⇌ C + D is considered in this work, where component C is considered the desired product and component D is considered the by-product. When working at the proof-of-concept stage, it is common to use a general case. For example, Melles et al. [35] considered a generic reaction A + B ⇌ C with various stoichiometries, and Sundmacher and Qi [36] proposed different RD designs and compared the performances of the designs based on a general reaction A_1 ⇌ A_2. Another more commonly used general reaction is the reaction A + B ⇌ C + D [37,38], where Kaymak and Luyben [39] modified the chemical equilibrium and Cheng and Yu [40] varied the activation energy, pre-exponential factor, and relative volatility. Despite using general cases, the literature provided valuable information on the feasibility of using RD for the separation of various reactive systems and paved the road for the work of other researchers. Other than reactive systems, generic cases are also used when developing other novel designs, such as the novel liquid-only transfer dividing wall columns proposed by Agrawal [41] and Agrawal [42].

Reactions with both low and high chemical equilibrium are considered in this work, and the general input variables (e.g., binary interaction parameters, chemical equilibrium) applicable to both cases are summarised in Table 1. Multiflash [43], along with the binary interaction parameters (BIPs) in Table 1, is used to obtain the component properties, where UNIQUAC is chosen to describe the liquid phase interactions while ideal gas is used for the vapour phase interactions. As shown in Table 1, the BIPs, described by the equation $A_{ij} = a_{ij} + b_{ij}T + c_{ij}T^2$ [43], for all component pairs are defined as zeros, except for the AC pair. With those BIPs, the mixture has only one minimum boiling azeotrope AC, and the boiling and azeotropic points of the mixture are as shown in Table 2. The boiling points of the components follow the order AC < C < A < D < B (low to high boiling points), and the azeotropic point is at (0.447, 0.553) mol mol^{-1} A and C. Other than the BIPs, some other parameters (e.g., activity coefficients, vapour pressures, enthalpies) are also required to complete the thermodynamic properties of a component. For simplicity, real components are used as the basis, where component A uses the data from ethanol, component B from acetic acid, component C from ethyl acetate, and component D from water. Other real components can of course also be considered as long as they have the same characteristics as outlined above. Although the mixture is derived from real component thermodynamic data, it is inherently an artificial system, and the artificial system is only used to illustrate the technical feasibility of a highly integrated and intensified HRDWC.

After defining the reaction mixture, the reaction kinetics should be defined. A few assumptions are made regarding the reaction:

1. The reaction is heterogeneously catalysed, but a pseudo-homogeneous model can describe the reaction rate [44].
2. The reaction occurs only in the liquid phase as the vapour holdup at each stage is negligible.
3. The reaction rate is based on the liquid volume at each stage in the RD column, and it is assumed that the liquid volume per stage is 0.1 m^3 [9]. A discussion of the effect of the liquid holdup can be found in [9].

According to Assumption 1, the forward and backward reaction rates can be described with the Arrhenius law:

$$r_f = k_{f0} \exp\left(\frac{-E_{a,f}}{RT}\right) C_A C_B \tag{2}$$

$$r_b = k_{b0} \exp\left(\frac{-E_{a,b}}{RT}\right) C_C C_D \tag{3}$$

where r_f and r_b are the forward and backward reaction rates (kmol m^{-3} s^{-1}), k_{f0} and k_{b0} are the forward and backward pre-exponential factors (m^3 $kmol^{-1}$ s^{-1}), $E_{a,f}$ and $E_{a,b}$ are the forward and backward activation energies (kJ mol^{-1}), R is the gas constant (J K^{-1} mol^{-1}), T is the temperature (K), and C_i, where $i \in \{A, B, C, D\}$, are the concentrations of components A, B, C, and D (kmol m^{-3}), respectively. The forward and backward activation energies are assumed to be the same in this work, where $E_{a,f} = E_{a,b} = 80$ kJ mol^{-1} [9].

This work considers two cases of low and high chemical equilibrium, i.e., conversions, respectively, and these are manipulated by changing the chemical equilibrium (K_{eq}) so that $K_{eq} = 0.184$ for the low conversion case and $K_{eq} = 81$ for the high conversion case, obtained from our previous work, where the low and high K_{eq} values correspond to a single pass reaction conversion of 30% and 90%, respectively [9]. Then, according to $K_{eq} = k_{f0}/k_{b0}$ and by fixing k_{f0}, the values for k_{b0} can be calculated for both cases. For both low and high chemical equilibrium cases, the fresh (i.e., pure) reactants A and B are provided at a rate of 12.6 kmol h^{-1} [9], and both feed streams are assumed to be provided at 1 atm as saturated liquids.

4. Optimal results

As mentioned in Section 2.3, the optimisation problem in this work is a MINLP problem, and the problem is solved using Genetic Algorithm (GA) and Particle Swarm Optimisation (PSO), which are both categorised as stochastic optimisers. Details of the GA and PSO settings used were provided in Section 2.3. The optimisation is solved on a workstation equipped with a dual Intel Xeon Gold 6226R CPU with 32 cores (64 processors) and 2.9 GHz clock speed, and the total RAM capacity is 192 GB (3200 MHz). To speed up the optimisation, 54 workers are used for parallel computing adopting a master–slave structure. A single design optimisation may take up to three hours with

Table 1
General inputs for all case studies for the A + B ⇌ C + D reaction with AC forming a minimum boiling azeotrope.

Items	Values	Units
Thermodynamic model	UNIQUAC (liquid); Ideal gas (vapour)	–
Binary interaction parameters ($A_{ij} = a_{ij} + b_{ij}T + c_{ij}T^2$)		
a for AC pair	$a_{AC} = 471.244$; $a_{CA} = 2563.53$	J mol^{-1}
b for AC pair	$b_{AC} = -2.81123$; $b_{CA} = -1.90749$	J mol^{-1}
c for AC pair	$c_{AC} = c_{CA} = 0$	J mol^{-1}
a, b, c for every other pair	0	J mol^{-1}
Reaction kinetics (refer to Eqs. (2) and (3)**, and** $K_{eq} = k_{f0}/k_{b0}$)		
Activation energy, E_a	$E_{a,f} = E_{a,b} = 80$	kJ mol^{-1}
Chemical equilibrium, K_{eq}	0.184 (low); 81 (high)	–
Pre-exponential factor (forward), k_{f0}	1.682×10^7	m^3 kmol^{-1} s^{-1}
Reactant feed		
Flow rate, F	$F_A = F_B = 12.6$	kmol h^{-1}
Pressure, P	$P_A = P_B = 1$	atm
Vapour fraction, VF	$VF_A = VF_B = 0$ (saturated liquid)	–

Table 2
Boiling points and azeotropic points for the components and azeotropes involved in the mixture at 1 atm.

Comp.	Boiling point (°C)	Azeotropic point (mol mol^{-1})
AC	71.8	(0.447, 0.553)
C	77.2	–
A	78.3	–
D	100.0	–
B	118.0	–

parallel computing, depending on the complexity of the design. An optimisation problem is repeated several times (e.g., five times) using each optimisation method, and the solution with the best objective function is chosen as the final result.

Generally, the variables considered for optimisation of a distillation column Cn are the total number of stages (N_{tn}), kth feed stage location ($N_{fn,k}$), start and end stages of the reactive zone ($N_{\text{rxn,start/end}}$; for RD column C1), kth liquid side draw location ($N_{\text{sl}n,k}$; for the main column C3 in the DWCs), top liquid/vapour thermal coupling stream locations ($N_{\text{tc}n,\text{topL/V}}$; for the main column C3 in the DWCs), bottom liquid/vapour thermal coupling stream locations ($N_{\text{tc}n,\text{botL/V}}$; for the main column C3 in the DWCs), distillate or bottom flow rate (D_n or B_n) (but obviously not both so as not to violate the mass balance), kth side liquid/vapour flow rate ($F_{\text{sl}n,k}$ or $F_{\text{sv}n,k}$; for RDWC and HRDWC structures), and the reflux ratio (RR_n). The meaning of the symbols can be found in the nomenclature, and the full set of optimisation variables for each structure can be found in Table 3. An example flowsheet for RDWC-PS-Mid labelled with the optimisation variables is provided in Figure S2.1 in the supplementary material for clarification. For the RD-PS and RDWC-PS-Mid designs, the outlet pressure of the pump (P_{pump}; i.e., the pressure of the high-pressure column C4) is also optimised. It should be noted that the operating pressures of the other columns, including DWCs, are not optimised but fixed at atmospheric pressure (i.e., no pressure drop).

For the hybrid designs, RD-DP and HRDWC-DP-Mid, the membrane network needs to be optimised, thus adding additional degrees of freedom such as the number of membrane stages connected in series (N_{ms}), the number of membrane modules connected in parallel in a membrane stage n ($N_{\text{mm},n}$), (note that in this work the maximum number of stages is considered to be 8, i.e., $N_{\text{ms}}^{\max} = 8$), and the existence of a membrane stage feed heater before each membrane stage. To ease the optimisation burden, it was fixed a priori that the membrane stage feed heaters for each design will exist only between membrane stage two and the optimal membrane stage N_{ms}, i.e., not for the first membrane stage, because:

1. According to the findings in our previous work [13], in almost all the cases studied (a total of 24 cases studied), a membrane feed stage heater is likely to be present in front of all existing membrane stages.

Table 3
Low chemical equilibrium — Optimisation variables involved in each structure. Note that for hybrid structures involving membranes, the maximum number of membrane stages is defined to be 8 stages. See nomenclature for the meaning of the symbols. An example flowsheet for RDWC-PS-Mid labelled with the optimisation variables are given in Figure S2.1 in the supplementary material.

No.	RD-PS	RDWC-PS-Mid	RDWC-PS-Bot	RD-DP	HRDWC-DP-Mid	HRDWC-DP-Bot
1	N_{t1}	N_{t1}	N_{t1}	N_{t1}	N_{t1}	N_{t1}
2	$N_{f1,1}$ [a]	$N_{f1,1}$ [a]	$N_{f1,1}$ [a]	$N_{f1,1}$ [a]	$N_{f1,1}$ [a]	$N_{f1,1}$ [a]
3	$N_{f1,2}$ [a]	$N_{f1,2}$ [a]	$N_{f1,2}$ [a]	$N_{f1,2}$ [a]	$N_{f1,2}$ [a]	$N_{f1,2}$ [a]
4	$N_{f1,3}$	$N_{f1,3}$	$N_{f1,3}$	$N_{f1,3}$	$N_{f1,3}$	$N_{f1,3}$
5	$N_{\text{rxn,start}}$	$N_{\text{rxn,start}}$	$N_{\text{rxn,start}}$	$N_{\text{rxn,start}}$	$N_{\text{rxn,start}}$	$N_{\text{rxn,start}}$
6	$N_{\text{rxn,end}}$	$N_{\text{rxn,end}}$	$N_{\text{rxn,end}}$	$N_{\text{rxn,end}}$	$N_{\text{rxn,end}}$	$N_{\text{rxn,end}}$
7	B_1	N_{t2}	B_1	B_1	N_{t2}	B_1
8	RR_1	$N_{f2,1}$	N_{t2}	RR_1	$N_{f2,1}$	N_{t2}
9	N_{t2}	B_2	$N_{f2,1}$	N_{t2}	B_2	$N_{f2,1}$
10	$N_{f2,1}$	RR_2	B_2	$N_{f2,1}$	RR_2	B_2
11	B_2	N_{t3}	RR_2	B_2	N_{t3}	RR_2
12	RR_2	$N_{f3,1}$ [c]	N_{t3}	RR_2	$N_{f3,1}$ [c]	N_{t3}
13	N_{t3}	$N_{f3,2}$ [c]	$N_{f3,1}$ [c]	N_{t3}	$N_{f3,2}$ [c]	$N_{f3,1}$ [c]
14	$N_{f3,1}$ [b]	$N_{f3,3}$	$N_{f3,2}$	$N_{f3,1}$	$N_{\text{sl3,1}}$ [c]	$N_{\text{sl3,1}}$ [c]
15	$N_{f3,2}$ [b]	$N_{\text{sl3,1}}$ [c]	$N_{\text{sl3,1}}$ [c]	D_3	$N_{\text{sl3,2}}$	$F_{\text{sl3,1}}$ [c]
16	D_3	$N_{\text{sl3,2}}$	$F_{\text{sl3,1}}$ [c]	RR_3	$N_{\text{sv3,1}}$ [c]	D_3
17	RR_3	$N_{\text{sv3,1}}$ [c]	D_3	N_{ms}	$F_{\text{sl3,1}}$ [c]	RR_3
18	N_{t4}	$F_{\text{sl3,1}}$ [c]	RR_3	$N_{\text{mm,1}}$	$F_{\text{sl3,2}}$	N_{ms}
19	$N_{f4,1}$	$F_{\text{sl3,2}}$	N_{t4}	$N_{\text{mm,2}}$	$F_{\text{sv3,1}}$ [c]	$N_{\text{mm,1}}$
20	B_4	$F_{\text{sv3,1}}$ [c]	$N_{f4,1}$	$N_{\text{mm,3}}$	D_3	$N_{\text{mm,2}}$
21	RR_4	D_3	B_4	$N_{\text{mm,4}}$	RR_3	$N_{\text{mm,3}}$
22	P_4	RR_3	RR_4	$N_{\text{mm,5}}$	N_{ms}	$N_{\text{mm,4}}$
23	P_{pump}	N_{t4}	P_4	$N_{\text{mm,6}}$	$N_{\text{mm,1}}$	$N_{\text{mm,5}}$
24	–	$N_{f4,1}$	P_{pump}	$N_{\text{mm,7}}$	$N_{\text{mm,2}}$	$N_{\text{mm,6}}$
25	–	B_4	–	$N_{\text{mm,8}}$	$N_{\text{mm,3}}$	$N_{\text{mm,7}}$
26	–	RR_4	–	–	$N_{\text{mm,4}}$	$N_{\text{mm,8}}$
27	–	P_4	–	–	$N_{\text{mm,5}}$	–
28	–	P_{pump}	–	–	$N_{\text{mm,6}}$	–
29	–	–	–	–	$N_{\text{mm,7}}$	–
30	–	–	–	–	$N_{\text{mm,8}}$	–

[a] $N_{f1,1}$ is feed stage for component A, $N_{f1,2}$ is feed stage for component B.
[b] $N_{f3,1}$ is distillate from column C1, $N_{f3,2}$ is distillate from column C4.
[c] $N_{f3,1}$ is the top vapour thermal coupling stream of column C3;
$N_{f3,2}$ is the bottom liquid thermal coupling stream of column C3;
$N_{\text{sl3,1}}$ is the top liquid thermal coupling stream of column C3;
$N_{\text{sv3,1}}$ is the bottom vapour thermal coupling stream of column C3;
$F_{\text{sl3,1}}$ is the flow rate of the top liquid thermal coupling stream of column C3;
$F_{\text{sv3,1}}$ is the flow rate of the bottom vapour thermal coupling stream of column C3.

2. The distillate of column C3 (i.e., the feed stream to the membrane network) is at a temperature higher than the maximum allowable temperature for the membrane, here 70 °C [45]. Therefore, a membrane feed cooler is needed to cool the distillate to 70 °C. Also, according to Bausa and Marquardt [46], the performance of the pervaporation membrane is better at a higher temperature, so the membrane feed stage heater for the

first membrane stage can be omitted as the distillate is already at the highest tolerable temperature of the membrane after passing the membrane feed cooler.

The pressure of the membrane feed pump (i.e., retentate side pressure) is fixed at 5 atm so that the distillate will maintain in liquid phase even after heating by the membrane feed stage heaters [47]. The permeate side pressure for each membrane module is fixed at 400 Pa (0.0039 atm) [45]. Although these two pressures are fixed for this study, they could of course be added to the optimisation problem. The largest problem (i.e., HRDWC-DP-Mid) involves 30 decision variables, of which 23 are discrete variables (i.e., number of column and membrane stages, and feed locations) and 7 are continuous variables (i.e., flow rates and reflux ratios).

It should be noted that some of the optimisation variables stated in Table 3 are dependent on other variables. An equation can be used to relate the dependent variables, thus leaving only the independent variables to be optimised. For example, according to the findings in Section S1 in the supplementary material, the start of the reactive zone can be set equal to the feed location of the heavy reactant stream. Therefore, $N_{\text{rxn,start}} = N_{f1,2}$, so either $N_{\text{rxn,start}}$ or $N_{f1,2}$ will be chosen as the independent optimisation variable and the value of the other (dependent) optimisation variable will then be directly equal to it. The same principle is also applied to the pressure of column C4 (P_4) and pump before column C4 (P_{pump}) as these are considered equal.

There are a few constraints (i.e., design specification and/or process requirement) involved in the optimisation task, which are summarised below:

1. **Product specification: 99 mol% of component C in its product stream**
   In this case study, two products are generated from the reaction, and the ideal case would be to recover both products at high purity. To achieve high purity of both products, the design must fully recycle the non-reacted reactants and there needs to be an almost complete conversion for both reactants. However, this is very challenging, especially for reactions with low chemical equilibrium in an RD column. Moreover, in practice, by-products will often be produced in a reaction. Therefore, in this work, only component C, which forms an azeotrope with reactant A, is treated as the desired product (i.e., component D is treated as a by-product that will go into a waste stream) and the product specification is 99 mol% of component C in the product stream. Waste treatment cost is applied for the waste stream, which will be discussed later in relation to the costings.
2. **Dividing wall structure: Equal number of stages on both sides of the wall**
   In a DWC, the total pressure drop from the start to the end of the dividing wall will be the same on both sides of the wall (i.e., operating pressure on both sides of the wall at both ends should be the same), and this will impact on the vapour stream split across the wall. However, since no pressure drop is assumed in this case study, instead of restricting the total pressure drop on both sides of the walls to be the same, the constraint used in this work is that the number of stages on both sides of the wall is the same. (It is perfectly possible to consider the pressure drop in the column, and to optimise this, but given the complexity of the optimisation in this work this was not considered).
3. **Membrane feed: Composition of components B and D should be $\leq$ 0.0001 mol mol^{-1}**
   A constraint is imposed on the maximum composition of the heavier components into the membrane network because, in the structures proposed, the purpose of the membrane is only the break the azeotrope AC by allowing component A to permeate through the membrane (i.e., retaining purified component C in the retentate). If the other two components (B and D) are present in the membrane feed, an additional distillation column may be required to further purify the retentate to obtain product C that satisfies the product specification which is clearly not beneficial.
4. **Theoretical recovery** (β): $\beta \geq 0.8$
   The theoretical recovery (β) is an additional variable considered in this work, which is defined as:

$$\beta = \frac{\text{Molar flow rate of product C in the product stream}}{\text{Molar flow rate of reactant A in the feed}} \tag{4}$$

   The molar flow rate of reactant A in the feed considered in this work 12.6 kmol h^{-1}. The value of β can vary between 0 and 1, indicating the overall performance of reaction conversion and separation ($\beta = 1$ means complete conversion of both reactants and complete separation between the products). This work requires $\beta \geq 0.8$ to avoid cases where the amount of product is very small, leading to a low production-based total annualised cost (the objective function) defined in Eq. (5). Instead of setting a constraint on β, one can also set a minimum value for the molar flow rate of the product C to achieve the same effect. In this work, no optimisations hit this bound (0.8), which shows that this constraint does not limit the optimal designs (i.e., this constraint is inactive in this work).

The objective function for the optimisation is to minimise the production-based TAC subject to the product purity constraint in the final product stream and a theoretical recovery of at least 80 mol% (recall that component C is the only desired product). The production-based TAC can be expressed as:

$$\text{Production-based TAC (M \$ kg}^{-1}) = \frac{\text{Annualised CAPEX (M \$ y}^{-1}) + \text{OPEX (M \$ y}^{-1})}{\text{Mass flow rate of the product stream (kg y}^{-1})} \tag{5}$$

The capital cost (CAPEX) includes the cost of the column shells and column trays where the cost of reactive trays is assumed to be five times the cost of conventional (non-reactive) trays [48], reboilers, condensers, pumps, heaters/coolers, and membranes. The detailed equations for calculating the capital costs related to the distillation column and membrane network can be found in [13,49], respectively. The operating cost (OPEX) includes the cost of the utilities (heating/cooling/electricity), membrane replacement cost (where applicable) assuming a membrane lifetime of 2 years, and the organic waste treatment. It should be noted that the type of utility (e.g., low-/medium-/high-pressure steam) is automatically chosen during optimisation based on the temperature of the process stream exiting the heater/cooler and the minimum temperature approach ($\Delta T = 10$ K). The calculation of the organic waste treatment cost is based on the mass of components A, B, and C (component D is assumed to be non-organic) in the waste stream [9].

In the following sections, detailed separation and economic analysis will be performed. A detailed analysis reveals the feasibility of a process both from a technical and economic perspective, which is an important step to validate a concept. Moreover, the detailed results allow insights into the process, such as understanding the energy consumption and the cost drivers. These insights can unveil the advantages and limitations of a process so actions can be taken to enhance its benefits or to improve the process. The detailed analysis unravels the opportunities or challenges that may arise in a real-world application (e.g., can the process be retrofitted?) and demonstrates the economic potential of the processes (e.g., how much cheaper is a process when compared to others?). Although artificial components are used, comparing the separation and economic performances of the processes is fair because the modelling, equipment sizing, and cost equations are the same.

4.1. Low chemical equilibrium

This section will first compare the two base designs of either the RD-PS or RD-DP process. Next, we will compare the base designs (i.e., RD-PS and RD-DP) and their dividing wall modifications with the wall in the middle or extended to the bottom (e.g., RDWC-PS-Mid and RDWC-PS-Bot). Initially, low chemical equilibrium is considered (i.e.,

Table 4
Low chemical equilibrium — Optimal designs for reactive distillation (RD) and its reactive dividing wall column (RDWC)/hybrid reactive dividing wall column (HRDWC) counterparts with pressure swing (PS) and distillation-pervaporation (DP). -Mid indicates the dividing wall is in the middle of the column, and -Bot indicates the dividing wall column is extended to the bottom of the column. For variables with multiple values, they follow the sequence as reported in Table 3 (e.g., Feed stages = $N_{f1,1}/N_{f1,2}/N_{f1,3}$).

Item	RD-PS	RDWC-PS-Mid	RDWC-PS-Bot	RD-DP	HRDWC-DP-Mid	HRDWC-DP-Bot	Units
Column C1							
Total stages	40	32	36	42	31	40	–
Feed stages	21/8/31	18/6/20	17/5/22	24/9/39	18/4/24	21/7/37	–
Reactive stages	8/34	6/29	5/31	9/36	4/29	7/33	–
Bottom	35.61	124.71	46.75	33.78	133.32	37.00	kmol h^{-1}
Reflux ratio	1.35	–	–	1.31	–	–	mol mol^{-1}
Reboiler duty	847	–	1254	789	–	813	kW
Condenser duty	−886	–	–	−828	–	–	kW
Column C2							
Total stages	25	25	26	24	30	24	–
Feed stage	18	18	20	18	25	19	–
Bottom	21.68	30.99	32.79	19.84	29.01	23.17	kmol h^{-1}
Reflux ratio	1.81	1.75	1.98	1.69	1.96	1.95	mol mol^{-1}
Reboiler duty	426	419	453	408	446	445	kW
Condenser duty	−424	−417	−450	−405	−444	−443	kW
Column C3							
Total stages	26	48	51	27	50	53	–
Feed stages	12/17	13/46/10	15/10	16	14/46	13	–
Side liq. stage	–	13/38	15	–	14/17	13	–
Side vap. stage	–	46	–	–	46	–	–
Side liq.	–	50.75/22.81	67.15	–	59.63/16.91	47.18	kmol h^{-1}
Side vap.	–	86.23	–	–	100.08	–	
Distillate	29.87	35.23	36.33	21.09	21.29	21.05	kmol h^{-1}
Reflux ratio	1.97	3.50	3.14	2.03	5.16	4.90	mol mol^{-1}
Reboiler duty	753	1352	8	602	1194	316	kW
Condenser duty	−836	−1495	−1418	−603	−1235	−1170	kW
Column C4							
Total stages	26	25	21	–	–	–	–
Feed stage	14	10	8	–	–	–	–
Bottom	11.26	11.19	11.24	–	–	–	kmol h^{-1}
Reflux ratio	1.90	1.00	0.86	–	–	–	mol mol^{-1}
Reboiler duty	563	533	531	–	–	–	kW
Condenser duty	−415	−370	−352	–	–	–	kW
Pump							
Pressure	11.25	10.05	11.11	–	–	–	atm
Power	0.84	0.88	1.01	–	–	–	kW
Membrane network							
No. mem. stages[a]	–	–	–	4	5	5	–
No. mod. in stage 1	–	–	–	13	9	12	–
No. mod. in stage 2	–	–	–	15	10	11	–
No. mod. in stage 3	–	–	–	16	12	8	–
No. mod. in stage 4	–	–	–	25	9	12	–
No. mod. in stage 5	–	–	–	–	22	19	–
Total no. mod.	–	–	–	69	62	62	–
Total mem. area	–	–	–	414	372	372	m^2
Mem. heating duty	–	–	–	124	126	124	kW
Perm. cooling duty	–	–	–	−132	−134	−131	kW
Perm. heating duty	–	–	–	38	38	37	kW
Total duty							
Heating	2589	2304	2247	1961	1805	1736	kW
Cooling	−2561	−2282	−2220	−1968	−1813	−1743	kW

[a] The upper bound for the number of membrane stages is 8.

the backward reaction rate is significantly higher than the forward reaction rate; see Table 1 for input details). The design parameters, energy consumption, CAPEX, OPEX, and production-based TAC will be compared in separate sections. The optimal designs and cost information for each structure are shown in Tables 4 and 5, respectively. Note that for cases with low chemical equilibrium, the composition of the distillates of column C1 is located at the left-hand side of the azeotropic point (refer to Fig. 1 for the x-y diagram).

4.1.1. Design comparison

A comparison between the base designs, i.e., RD-PS and RD-DP, showed that their column C1 to C3 have similar designs. For example, comparing the total number of stages in columns C1, C2, and C3 for RD-PS vs RD-DP are 40 vs 42, 25 vs 24, and 26 vs 27, respectively. Other operating variables such as bottom/distillate flow rates, reflux ratios, and feed locations are similar (refer to Table 4 for the values). The similarities in the column designs indicate that the RD-PS and RD-DP designs can be retrofitted into one another by replacing column C4 (the high-pressure column of the PS system) with a membrane network and vice versa.

Comparing RD-PS and its dividing wall variations (RDWC-PS-Mid and RDWC-PS-Bot), looking at column C3 in the RD-PS structure, it can be seen that the distillate from column C1 is fed at stage 12 of C3, meaning that roughly 12 stages are required to separate the azeotrope in the distillate of column C1. Also, the design requires 40 stages in column C1. In the dividing wall designs, RDWC-PS-Mid and RDWC-PS-Bot, column C1 is to the left of the wall (prefractionator) while column

C3 is to the right (the main column), and the DWC (columns C1 + C3 together) will perform the reaction and separation tasks similarly to columns C1 and C3 in the base design (i.e., RD-PS). Therefore, the number of stages required by the main column (column C3) in the dividing wall variations is larger (48 stages for RDWC-PS-Mid and 52 stages for RDWC-PS-Bot, respectively) than that of RD-PS, as the main column integrates both columns C1 and C3 from RD-PS into a column shell (thus requiring roughly 40 (column C1 in RD-PS) + 12 (top of column C3 in RD-PS) = 52 stages). Although the dividing wall variations require more stages, all three designs actually require a similar number of stages for the top of column C3 (i.e., above the first feed location). Also, unsurprisingly, the reflux ratios of the main column C3 in the dividing wall variations are larger than RD-PS, as the reflux in the main column needs to be sufficient to cover the liquid flow requirement on both sides of the wall.

Looking at the feed stages of column C3, where the first two feeds are the start and end of the dividing wall (i.e., the top and bottom thermal coupling locations), and the last feed is the recycle from column C4, in RDWC-PS-Mid, it can be noted that the wall extends from stage 13 to stage 46 in a column with a total of 48 stages. Note that the column structures (e.g., RD-PS, RDWC-PS-Mid, or RDWC-PS-Bot) are fixed a priori as the focus of the optimisation in this work is not a superstructure optimisation of the column structures. This means that for RDWC-PS-Mid, there is a constraint that the dividing wall can never extend to the end of the distillation column (i.e., at least one (normal) stage is present at the end of the dividing wall). On the other hand, for RDWC-PS-Bot, the dividing wall always extends to the end of the distillation column. Therefore, the fact that the wall in RDWC-PS-Mid extends to nearly the end of the main column may indicate that the RDWC-PS-Bot structure is preferred.

Moving on to the dividing wall designs involving a membrane network to split the azeotrope. From a comparison between the RD-DP and its dividing wall counterparts (HRDWC-DP-Mid and HRDWC-DP-Bot), it can be seen that the configurations of column C2 and the membrane network are fairly similar between all three column structures. Similarly to the findings when comparing RD-PS and its dividing wall variations, the number of stages in column C3 for HRDWC-DP-Mid and HRDWC-DP-Bot is larger than that of RD-DP, and HRDWC-DP-Mid has its wall again extended to nearly the end of its main column (wall ending at 46 stages out of 50 stages).

An overall comparison shows that the corresponding pairs (i.e., RD-PS vs RD-DP, RDWC-PS-Mid vs HRDWC-DP-Mid, and RDWC-PS-Bot vs HRDWV-DP-Bot) have similar structures in terms of the number of stages, feed locations, flow rates, and reflux ratios, indicating that it is possible to retrofit one structure to the other by just switching between using an additional column (column C4) or a membrane network at the distillate of column C3. The slightly higher distillate in C3 for RD-PS is due to the recycling of the azeotrope from column C4, which does not exist in the RD-DP structure.

4.1.2. Energy comparison

Considering the energy consumption of the two base structures, RD-DP saves about 24% heating energy and 23% cooling energy (refer to Table 4), mainly due to the membrane network, compared to reactive distillation followed by pressure swing operation (RD-PS). Considering only the additional unit in RD-PS (column C4) and RD-PD (membrane network), the membrane network saves 63% heating energy and 68% cooling energy compared to the column (C4). However, it should be noted that the energy quality of the cooling is not the same, i.e., utility type is automated in the simulation based on the temperature of the target stream, and the cooling source for the condenser in C4 is cooling water while permeate cooling requires refrigerant (−50 °C), which leads to a higher cooling cost in RD-DP, which will be discussed later.

The comparison between RD-DP and the two corresponding dividing wall structures shows some reduction in energy consumption for the dividing wall structures, up to 13% drop for heating and cooling. It should be noted that, theoretically, the dividing wall structure with the wall extended to either the top or bottom should have similar consumption to their conventional counterpart [50], which is also reflected in our previous work on HDWC designs [12]. However, in this work, energy saving is observed for RDWC-PS-Bot due to the higher number of stages in the main column (51 stages for C3 in RDWC-PS-Bot) compared with its original design (26 stages for C3 in RD-PS), as a design with more stages requires less vapour from the reboiler (i.e., energy consumption). In our previous work [12], the number of stages in the prefractionator and the main column were found to be very close to the number of stages of their corresponding columns in the base design. It should be noted that the system considered in [12] was a binary mixture without reactions.

For RDWC-PS-Bot, the reboiler duty of C3 is very small (8 kW) compared with its condenser duty (−1418 kW), This is because the feed stream from C1 to C3 is pure vapour (recall that it is a thermal coupling stream), and the feed stream from C4 is vaporised through the valve (recall that it is changed from high pressure (11.11 atm) to atmospheric pressure) and contains 0.48 $kg\,kg^{-1}$ vapour. Therefore significantly lower energy is required in the reboiler to ensure the energy transfer between liquid and vapour flow in the column. Moreover, the main separation happens above the feed (rectifying section) i.e., the composition profile after the feed remains almost constant, reducing the need for reboiler energy. A similar case is also found for HRDWC-DP-Bot.

It is also worth noting that the dividing wall design with the wall in the middle (RDWC-PS-Mid) does not save energy compared with the design with the wall extended to the end (RDWC-PS-Bot), which indicates that the mixing and remixing effect are not reduced. In principle, a DWC with the wall installed in the middle allows the middle boiling component to be freely distributed, which helps the temperature and composition profile developed in the main column to reduce the mixing and remixing effect. For the case in this work, the middle boiling component A (recall that the lightest component C forms the minimum-boiling azeotrope with A) would be freely distributed on both sides of the wall, and, as the mixture is located at the left-hand side of the azeotropic point (see Fig. 1), pure A will be withdrawn in the sidedraw from the main column (C3) and recycled back to the prefractionator (C1), while the heavier components B and D will leave the DWC in the bottom stream and be further processed in column C2. However, due to (1) the low chemical equilibrium; (2) a large difference between boiling points between the reactants; and (3) the feed stage of the heavy reactant being close to the top of the column, the top stream from the C1 column (the prefractionator) contains a moderate amount of the heavier components B and D (0.0936 $mol\,mol^{-1}$ and 0.1362 $mol\,mol^{-1}$, respectively), which destroys the composition development in the main column and does not achieve energy saving. In addition, the vapour split stage (i.e., end of the dividing wall) is very close to the bottom, which shows that the optimal design is likely to be RDWC-PS-Bot.

For the three structures with membrane networks, similar findings are found. For example, both dividing wall structures save heating and cooling energy, with savings up to 11%. The energy saving for HRDWC-DP-Bot, and why this structure is more energy efficient than HRDWC-DP-Mid, can be explained similarly to above. For the membrane network, the energy consumption for heating and cooling is almost identical, which is reasonable as the dividing wall modification does not change the reactions and separation principles. Thus the reaction conversion remains almost constant, and the amount of azeotrope separated from column C3 is similar (distillate is 21.05–21.29 $kmol\,h^{-1}$).

In terms of overall comparison between the six structures, it is clear that all hybrid structures involving a membrane network (DP structures) save energy compared with their corresponding PS structures, where RD-DP, RDWC-DP-Mid, and RDWC-DP-Bot save 24%, 21%, and 22% total energy, respectively. The total (heating + cooling) duty required by HRDWC-DP-Bot (3479 kW) is 32% less than RD-PS

Table 5
Low chemical equilibrium — Costing information for reactive distillation (RD) and its reactive dividing wall column (RDWC)/hybrid reactive dividing wall column (HRDWC) counterparts with pressure swing (PS) and distillation-pervaporation (DP). -Mid indicates the dividing wall is in the middle of the column, and -Bot indicates the dividing wall column is extended to the bottom of the column.

Item	RD-PS	RDWC-PS-Mid	RDWC-PS-Bot	RD-DP	HRDWC-DP-Mid	HRDWC-DP-Bot	Units
Capital cost (CAPEX)							
Column	2.7810	3.0718	3.2948	2.3840	2.9416	2.9534	M $
Membrane	–	–	–	2.2694	2.0392	2.0392	M $
Reboiler	0.9487	0.7589	0.8884	0.6912	0.5210	0.6581	M $
Condenser	0.7310	0.5916	0.5843	0.5392	0.4077	0.4004	M $
Others	0.0437	0.0438	0.0439	0.8828	1.0130	1.0127	M $
Operating cost (OPEX)							
Waste	0.2611	0.2732	0.2629	0.2628	0.2384	0.2429	M $ y^{-1}
Heating	1.1133	0.9916	0.9672	0.8333	0.7671	0.7377	M $ y^{-1}
Cooling	0.0274	0.0244	0.0238	0.0719	0.0711	0.0691	M $ y^{-1}
Electricity	0.0004	0.0004	0.0005	0.0001	0.0001	0.0001	M $ y^{-1}
Mem. Rep.	–	–	–	0.0635	0.0571	0.0571	M $ y^{-1}
Product (Component C, constraint = 99 mol%)							
Flow rate	11.26	11.19	11.24	11.26	11.39	11.37	kmol h^{-1}
Overall							
CAPEX	4.5043	4.4662	4.8113	6.7666	6.9224	7.0637	M $
Ann. CAPEX	0.5630	0.5583	0.6014	0.8458	0.8653	0.8830	M $ y^{-1}
OPEX	1.4022	1.2897	1.2544	1.2316	1.1338	1.1068	M $ y^{-1}
TAC	1.9653	1.8480	1.8559	2.0774	1.9991	1.9898	M $ y^{-1}
Prod. TAC	0.2369	0.2242	0.2242	0.2506	0.2384	0.2377	M $ kg^{-1}

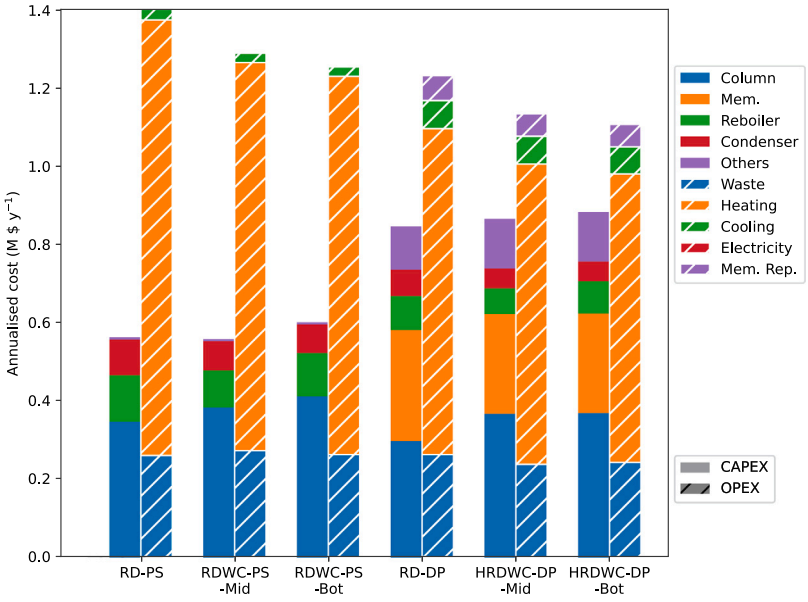

Fig. 5. Low chemical equilibrium — Stacked bar graph showing the breakdowns of the annualised capital cost (CAPEX) and operating cost (OPEX) for reactive distillation-pressure swing (RD-PS), reactive dividing wall column-pressure swing (RDWC-PS), reactive distillation-distillation-pervaporation (RD-DP), and hybrid reactive dividing wall column-distillation-pervaporation (HRDWC-DP). The suffix -Mid and -Bot indicate that the wall is in the middle and extended to the bottom, respectively.

(5150 kW). However, as previously mentioned, refrigerant (−50 °C) is used as a cooling utility in the membrane network, hence the cooling cost is higher for three DP structures. It should be noted that the results obtained are specific to the membrane considered in this work. A different membrane performance will of course have an impact on the relative benefits of this hybrid mode.

4.1.3. Cost comparison

The distribution and breakdown of the costs of the structures are given in Table 5 and also shown in Fig. 5 and Figure S3.1 (shown in supplementary material). From Fig. 5, in general, the CAPEX of the structures involving the membrane network (RD-DP, HRDWC-DP-Mid, and HRDWC-DP-Bot) are about 47% to 55% higher than the PS structures (RD-PS, RDWC-PS-Mid, and RDWC-PD-Bot). The higher capital cost in the DP variations is due to the expensive membranes used. If comparing only structures of the same category (PS variations or DP variations), it can be seen that the CAPEX of RDWC-PS-Bot and HRDWC-DP-Bot are slightly higher than their respective based case and -Mid variations. The main contributor to the higher CAPEX is the costs of the columns, as the columns (especially column C3) in RDWC-PS-Bot and HRDWC-DP-Bot have more stages when compared to their respective variations.

Considering the OPEX, Fig. 5 clearly shows that the OPEX of the DP structures are lower than those of PS structures, and this is consistent with findings in the literature [4–6]. It can also be seen that the heating cost is the most significant contribution (more than 50%) to each design, which ranges from 67% (HRDWC-DP-Bot) to 79% (RD-PS). From Table 5, looking at the waste treatment cost, it is clear that HRDWC-DP-Mid and HRDWC-DP-Bot have a lower cost due to the higher reaction conversion (i.e., higher product flow rate). As the

waste treatment is a function of the amount of organic waste (recall that components A, B, and C are treated as organic waste), higher overall conversion leads to less organic components in the waste stream and therefore lower waste treatment cost. Also, although the values are very small for the electricity costs, the PS structures require higher electricity costs than the DP structures because the PS structures use an electric pump to increase the pressure of the feed stream into the high-pressure column (C4). For the heating cost, it is not surprising that the DP structures have less cost due to the lower heating requirement. Moreover, the heating utility in column C4 requires medium-pressure steam (recall that the operating pressure in column C4 is above 11 atm), while other heating units only need low-pressure steam, which further increases the heating cost of the PS structures. For the cooling cost, although the DP structures require lower total cooling duty, the much more expensive refrigerant (−50 °C) utilised in the membrane network makes the DP structures cost more in terms of cooling. This could be improved by using a higher pressure on the permeate side of the membrane, so the refrigerant is no longer required, however, with a higher permeate side pressure, the separation performance of the membrane drops, therefore requiring more membrane stages and modules, leading to a higher capital cost. Note that in this work, the permeate pressure is considered fixed.

The objective function considered in this work is production-based TAC. Table 5 indicates that the best designs are the designs based on a dividing wall reactive column followed by PS operation (RDWC-PS-Mid and RDWC-PS-Bot). It can also be seen that the PS structures are slightly better than their corresponding membrane network (DP) structures with up to about 6% reduction (pair of RDWC-PS-Mid and HRDWC-DP-Mid). Also, the PI of the dividing wall structures can achieve minor cost savings for both PS and DP structures with about 5% savings. Considering the two types of dividing wall structures, the structure with the wall extended to the bottom (-Bot) is marginally better for both designs (if more decimal places are considered for PS structures), however, the biggest difference is only 0.3%, which is negligible. It should be noted that the final product flow rate in each optimal design is very close (11.19–11.39 kmol h^{-1}). Moreover, Fig. 5 and Figure S3.1 show that although the operating cost is the main cost contributor in each design (more than 50%), the contribution of the operating cost to the total annualised cost drops from about 71% (RD-PS) for the PS structures to 59% (RD-DP) for the DP structures, which is due to the energy saving for the DP structure (see energy discussion in Section 4.1.1).

It is worth noting that the results above are based on the given costing specifications, for instance, the operating year considered for the annualised capital cost is eight years. With increasing operating years, the DP structures will be more beneficial as they have lower OPEX (including the utility and membrane replacement costs), and the high CAPEX will be averaged to a smaller value. The condition will be reversed for reduced operating years.

4.2. High chemical equilibrium

Until now, we have considered the situation where the conversion of the reaction is low, and the results obtained are for that condition. Next, we will consider the opposite situation, that of high conversion. The conversion of the reactants will be larger for a reaction with higher chemical equilibrium, leading to a higher molar composition of the products in both distillate and bottom flows from the RD column.

Ideally, for a high chemical equilibrium reaction (A + B ⇌ C + D), an excess in one of the reactants could lead to the other reactant being almost completely consumed, which reduces the separation difficulty. Also, in the study by Muthia et al. [51], even without an excess of one of the reactants, a single RD column may be sufficient to achieve complete conversions of both reactants and to separate the two products. However, there may be cases where complete conversion cannot be achieved regardless of excess or non-excess reactants. Therefore, a pre-optimisation study should be carried out to determine the possible structures.

In the following, we will first consider three situations for a single RD column to explore the effects of the amount of the reactants (A in excess, B in excess, and equimolar). In the optimisations with an excess reactant (either A or B), the feed flow rate of the reactant that should be in excess is considered as an extra optimisation variable, and the objective function is to maximise the conversion of the non-excess reactant. The only constraint considered is that at least 90% of the product C generated should leave the column from the distillate to ensure a good separation performance. This constraint is reasonable as if a moderate amount of product C leaves from the bottom of the RD column, another distillation column would be required to separate it. For the optimisation, the upper bound on the total number of stages is 100 stages, and the reactive zone is optimised as before (range: stage 1 to stage 100). The feed flowrate of the non-excess reactant is set at 12.6 kmol h^{-1}, and the maximum allowed ratio between excess and non-excess reactants is 10 (i.e., the upper bound of the excess reactant is 126 kmol h^{-1}). For the equimolar case, both feed flow rates of A and B are set as 12.6 kmol h^{-1}. The optimal design for the equimolar case reaches a reaction conversion up to 78%. The cases with excess A or B increase the reaction conversion to 95% and 94%, respectively, but it still does not completely consume the non-excess reactants even with a very large number of stages (about 100 stages is reported by the optimiser for the case with excess A).

In this work, despite using excess reactants, a near-complete reaction conversion of the non-excess reactant cannot be achieved. Therefore, similarly to the case of low chemical equilibrium discussed in Section 4.1.1, recycling the non-reacted A and B is still required. However, the presence of the azeotrope complicates the discussion for high chemical equilibrium. For the cases with equimolar or excess B, the majority of A is consumed, so the composition of A and C in the distillate mixture will be located on the right-hand side of the azeotropic point (referring to the 1 atm curve on Fig. 1). (Note that for the low chemical equilibrium case, the composition of A and C in the distillate was located on the left-hand side of the azeotropic point at 1 atm.) For the case with excess A, if A is only slightly in excess in the RD column, then the composition of the mixture of A and C may still be located on the right-hand side of the azeotropic point (recall that the azeotropic molar composition is 0.553 of C). However, the composition may shift to the left-hand side of the azeotropic point if a large amount of excess A enters the RD column. If optimisation is considered, the amount of excess A can be represented by the recycle flow rate of A into the RD column. Then, depending on the recycle flow rate, the mixture can be located either at the right-hand side (slight excess) or at the left-hand side (large excess) of the azeotropic point, and those two cases will need a different distillation structure, thus leading to a superstructure optimisation problem. To simplify the presentation, the case with a large excess of A is not considered in this work, and our discussion will be directly limited by the structure developed only for cases where the composition of A and C in the mixture is at the right-hand side of the azeotropic point (see Fig. 6 and further discussion in subsequent paragraphs).

To handle the azeotropic mixture with a larger amount of component C (i.e., right-hand side of the azeotropic point), the PS structure for low chemical equilibrium (Fig. 2(a)) cannot be used directly. According to Fig. 1, the azeotropic point shifts to the left as the pressure increases thus making the right-hand region larger, meaning that if the azeotropic point is initially at the right-hand side at 1 atm (which is the case for the distillate of column C1), increasing the pressure will not make the mixture composition shift to the left-hand side of the azeotropic point, so only pure C and azeotrope AC will still be obtained (i.e., pure A cannot be obtained). To also obtain pure A, the distillate of column C1 (mixture at 1 atm and at the right-hand side of the azeotropic point) must first enter a high-pressure column (to obtain pure C and azeotrope at a new azeotropic point which is further to the left-hand

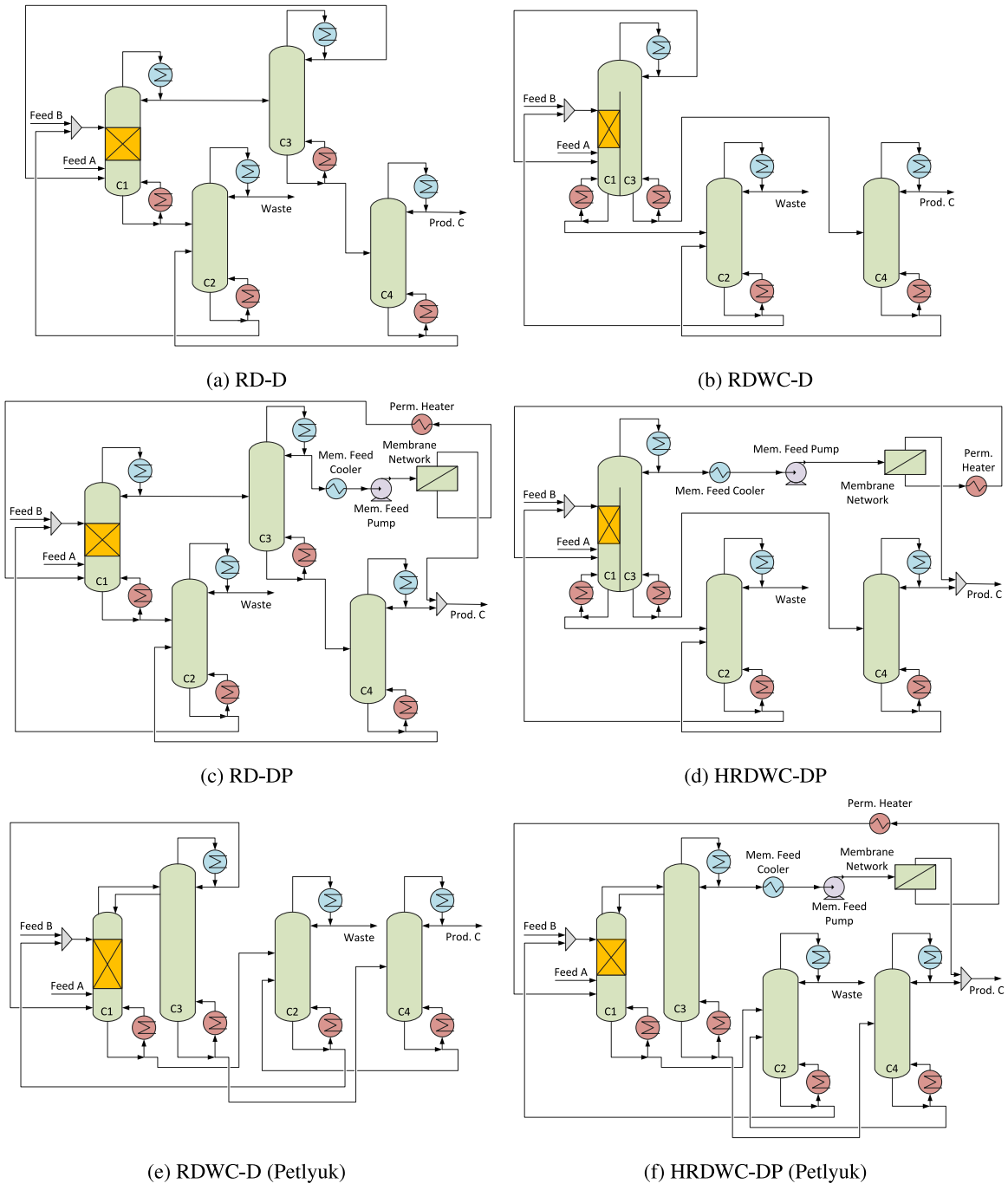

Fig. 6. High chemical equilibrium — Flowsheets of the reactive distillation (RD) and its reactive dividing wall column (RDWC) or hybrid reactive dividing wall column (HRDWC) counterparts with (a,b) conventional distillation column (D), and (c,d) distillation-pervaporation (DP). (e) and (f) are the Petlyuk structures used in simulations for (b) RDWC-D and (d) HRDWC-DP, respectively. Note that the dividing wall structures have the wall extended to the bottom of the main column. The detailed membrane network is shown in Fig. 3.

side) then a low-pressure column (the "left-hand side" azeotrope is now in the left-hand side region of the lower pressure, e.g., 1 atm, curve) to obtain pure A. However, this modification causes two potential problems for our analysis. First, if the column, whose feed stream is the distillate from the RD column C1, is operated under high pressure, then this column cannot form a dividing wall structure with the RD column (like the previous RDWC-PS structure in Fig. 2) unless the first column is also operated under the same high pressure, which will further complicate the study as the operating pressure in each column must then also be optimised. If the first column in the PS design is operated at atmospheric pressure (i.e., same as the RD column), then the second column in the PS design would need to be operated under vacuum, which would require additional considerations for the design and cost calculations. Secondly, without considering a large amount of excess A, the amount of unreacted A may be small, leading to a small amount of azeotropic formed. Therefore, applying the PS columns to handle the small amount of azeotrope may not be economically beneficial. Instead, this small amount of azeotrope may be considered as waste or recycled back into the RD column. This work aims to recycle as many unreacted reactants as possible so the azeotrope will be recycled back into the RD column. It should be noted that for the hybrid separation structure (involving DP), the azeotrope will be processed by a membrane network, hence the above problem is not present.

Following on from the discussion above, the base case for handling the high chemical equilibrium reaction is shown in Fig. 6(a) (reactive distillation with conventional distillation columns, RD-D). Like RD-PS or RD-DP for low chemical equilibrium shown in Figs. 2(a) and 2(d), the columns C1 and C2 in RD-D are responsible for reaction and recycling heavier boiling reactants, respectively. The feed to column C3 (i.e., distillate from the RD column C1) contains mostly product C and a small amount of other components. Since the composition of mixture A and C in the feed of column C3 is located on the right-hand side of the azeotropic point, the distillate of column C3 will contain a small amount of azeotrope near the azeotropic point, while the bottom flow will contain a large amount of product C and some B and D. Therefore, another distillate column C4 is required to process the bottom flow of column C3 to purify the product further and to recycle the unreacted reactant B. It should be noted that the bottom flow of column C4 contains both reactant B and by-product D, so the bottom stream should be recycled back to C2.

Also, like the dividing wall structures for low chemical equilibrium, C1 and C3 can be integrated into a single column with a dividing wall. The results from low chemical equilibrium showed that for the DWC structure with the wall in the middle, the wall was extended to nearly the end of the main column. Moreover, the corresponding production-based TACs for the dividing wall structures were very similar, thus implying that the structure with the wall extended to the end may be more desirable. Therefore, for simplification, in the high chemical equilibrium case, only the design with the wall extended to the bottom (see Fig. 6(b) for RDWC-D) is considered. The hybrid process using the membrane system (RD-DP, see Fig. 6(c)) has the same column sequences as for RD-D and the only difference is the membrane network used to separate the azeotrope into pure reactant A and product C, and this modification is also applied for the dividing wall structure (HRDWC-DP, see Fig. 6(d)). For RDWC-D and HRDWC-DP, due to the lack of the DWC packages in gPROMS, the thermodynamic equivalent Petlyuk structures (see Figs. 6(e) and 6(f) for RDWC-D and HRDWC-DP, respectively) are again used instead.

The same objective functions and constraints are also applied for the high chemical equilibrium, and the optimal designs and cost information are shown in Tables 6 and 7, respectively. Similar to the low chemical equilibrium case, the cost information is plotted in the bar (Fig. 7) and donut graphs (Figure S3.2 in supplementary material).

4.2.1. Design comparison

Starting with the comparison between RD-D and RD-DP, it can be seen that, while the number of stages are the same for column C2 (27 stages), the reflux ratio in RD-DP is almost halved when compared to RD-D (0.75 for RD-DP vs 1.46 for RD-D). This can be explained by the bottom stream composition from column C4 which is recycled back into column C2. The bottom stream composition of column C4 in RD-DP is about 0.95 mol mol^{-1} of the by-product D while it is about 0.80 mol mol^{-1} of D in RD-D, meaning that the separation task in RD-DP is easier when compared to RD-D, so a smaller reflux flow (thus smaller reflux ratio since their distillate flow rates are similar) is sufficient to establish the vapour–liquid equilibrium required in column C2 to separate the components. Moreover, when the bottom stream of column C4 is recycled back into column C2, the recycle location (i.e., the second feed stage of column C2 shown in Table 6) for RD-DP is near the top (stage 2) while for RD-D it is near the bottom (stage 20). The recycled stream is made up of saturated liquid, which can also act as a reflux flow. Therefore, the closer the recycle stage is to the top, the smaller the reflux ratio required to ensure a sufficient reflux flow to keep the stages above the uppermost feed stage (i.e., the recycle stage) from drying up. A similar argument can be used to explain the smaller reflux ratio required by column C2 in HRDWC-DP compared to that of RD-DP. Both the recycle stages in RD-DP and HRDWC-DP are close to the top, but because the recycle flow rate in HRDWC-DP is about twice that of RD-DP (not shown), the reflux ratio required by column C2 in HRDWC-DP is smaller than that of RD-DP.

Table 6
High chemical equilibrium — Optimal designs for reactive distillation (RD) and its reactive dividing wall column (RDWC)/hybrid reactive dividing wall column (HRDWC) counterparts with conventional distillation column (D) and distillation-pervaporation (DP). Note that the wall dividing wall structures have the wall extended to the bottom of the main column.

Item	RD-D	RDWC-D	RD-DP	HRDWC-DP	Units
Column C1					
Total stages	57	50	50	46	–
Feed stages[a]	54/7/29	48/6/32	44/9/47	44/10/38	–
Reactive stages[b]	7/51	6/47	9/44	10/43	–
Bottom	20.85	24.56	27.55	22.51	kmol h^{-1}
Reflux ratio	1.87	–	2.63	–	mol mol^{-1}
Reboiler duty	610.42	660.48	642.60	693.52	kW
Condenser duty	−650.73	–	−684.11	–	kW
Column C2					
Total stages	27	22	27	20	–
Feed stage[c]	23/20	20/15	20/2	17/4	–
Bottom	13.27	18.70	19.72	19.77	kmol h^{-1}
Reflux ratio	1.46	1.70	0.75	0.05	mol mol^{-1}
Reboiler duty	370.85	411.35	263.13	155.41	kW
Condenser duty	−369.84	−410.28	−261.86	−155.76	kW
Column C3					
Total stages	26	60	31	58	–
Feed stages	11	10	18	12	–
Side liq. stage	–	10	–	12	–
Side liq.	–	49.50	–	48.71	kmol h^{-1}
Distillate	6.07	4.45	6.81	5.40	kmol h^{-1}
Reflux ratio	3.35	19.74	2.53	16.98	mol mol^{-1}
Reboiler duty	246.48	162.92	221.62	177.50	kW
Condenser duty	−245.88	−862.79	−221.35	−910.39	kW
Column C4					
Total stages	26	28	24	28	–
Feed stage	15	18	16	19	–
Bottom	6.28	8.15	5.81	10.78	kmol h^{-1}
Reflux ratio	2.52	2.55	3.98	3.54	mol mol^{-1}
Reboiler duty	356.77	354.30	294.30	346.85	kW
Condenser duty	−358.37	−356.30	−295.08	−347.99	kW
Membrane network					
No. mem. stages[d]	–	–	3	3	–
No. mod. in stage 1	–	–	4	3	–
No. mod. in stage 2	–	–	3	5	–
No. mod. in stage 3	–	–	10	6	–
Total no. mod.	–	–	17	14	–
Total mem. area	–	–	102	84	m^2
Mem. heating duty	–	–	16.47	24.81	kW
Perm. cooling duty	–	–	−25.65	−30.53	kW
Perm. heating duty	–	–	7.23	8.80	kW
Total duty					
Heating	1584.52	1589.06	1445.36	1406.87	kW
Cooling	−1624.81	−1629.37	−1488.04	−1444.66	kW

[a] Feed for component A/Feed for component B/Distillate from column C3.
[b] Reactive section start/Reactive section end.
[c] Bottom stream from column C1/Bottom stream from column C4.
[d] The upper bound for the number of membrane stages is 8.

Next, we move on to comparing the base designs and their DWC counterparts (RD-D vs RDWC-D and RD-DP vs HRDWC-DP). In the high chemical equilibrium case, recall that we only consider the dividing wall structure where the wall is extended to the bottom. Similarly to the reason discussed in Section 4.1.1, the reflux ratio of the main column (column C3) of the dividing wall structures is significantly larger than that of the base structures, even though the number of stages is slightly lower, and this is because the reflux ratio in the dividing wall structures needs to be sufficiently large to cover the reflux flow on both sides of the wall.

Although not shown in the table, from the simulation results of the optimal designs it was found that the composition of by-product D in the bottom stream of column C4 in the hybrid structures is

higher (about 0.90 mol mol^{-1} in RD-DP and HRDWC-DP vs about 0.80 mol mol^{-1} is RD-D and RDWC-D), indicating that there is a possibility where the bottom stream of column C4 in RD-DP and HRDWC-DP can be directly treated as a waste stream (i.e., no need to recycle back into column C2). However, this finding may not be true if some of the design parameters change. Also, to consider the design without recycling the bottom stream of column C4, a superstructure needs to be formulated, which is beyond the scope of this investigation as previously stated.

An overall like-for-like comparison (i.e., RD-D vs RD-DP and RDWC-D vs HRDWC-DP) shows that the column designs (total number of stages, distillate/bottom flowrates, and reflux ratio) are similar. Coupled with the fact that the separation tasks (i.e., functions) of each column in the different designs are the same (e.g., column C1 in RD-D and RD-DP is used to separate mainly components A and C at the distillate and components B and D at the bottom), indicates that one design can be retrofitted into another design by simply adding or removing the membrane network. This finding is also found in the case of low chemical equilibrium discussed in Section 4.1.1. The slight differences between the number of stages and feed locations can be rectified by modifying the distillate flow rate, reflux ratio, or the number of membrane stages (if a membrane network is involved).

4.2.2. Energy comparison

An overall energy comparison (shown in Table 6) shows that membrane network structures (RD-DP and HRDWC-DP) save energy compared with the standard structures (RD-D and RDWC-D) with up to 11% saving in heating and cooling. Although HRDWC-DP saves a small amount of energy compared with its base case (RD-DP), with about 3% saving in heating, the RDWC-D requires slightly more energy than RD-D. Considering the summation of energy consumption of columns C1 and C3 (these two columns are integrated into a single DWC in both process intensified structures), there is no obvious energy saving for either dividing wall structures compared with their corresponding base structures. Therefore, it could be deduced that applying the dividing wall structures for the reactive systems would not ensure better energy efficiency. As described in the previous section for low chemical equilibrium (Section 4.1), theoretically, the dividing wall structure with the wall extended to either end of the column could not reduce the energy consumption without considering the effects of the changing number of stages.

It should be noted that the energy consumption (reboiler duty and condenser duty) of column C2 for the DP structures is significantly lower compared with the standard structures. The discussion in Section 4.2.1 explained that for the DP structure, the composition of the second feed stream (bottom stream from C4) is a very pure component D, which should leave the system from the distillate of column C2. Therefore, the separation task in C2 is easier for DP structures leading to lower energy consumption.

Similar to the DP structures in the low chemical equilibrium case, the cooling utility used in the permeate cooler is refrigerant (−50 °C). However, the small amount of energy required, no more than −30.53 kW, does not largely affect the overall quality of the cooling energy. Based on this point, the membrane system may be potentially improved, and the detailed discussion can be found in Section 4.1.2.

4.2.3. Cost comparison

Table 7 and Fig. 7 show that the column cost for the standard dividing wall structure (RDWC-D) is lower than that of its base case (RD-D), while for the hybrid structures (RD-DP and HRDWC-DP) the column cost are similar. A more detailed analysis based on the individual column costs (not shown) did not show any definitive reason for the differences in costs. However, Table 7 and Fig. 7 clearly show that the column cost of the hybrid structures (RD-DP and HRDWC-DP) is lower when compared to the distillation-only structures (RD-D and RDWC-D). This is because in the hybrid structures, instead of directly recycling the distillate of column C3, which contains mainly azeotrope, back into column C1, the distillate of column C3 is sent to a membrane system to be further purified into pure reactant A and product C. Then, the retentate containing almost pure reactant A is recycled back into column C1. This will improve the separation and reaction performances of column C1 in the hybrid structures because not only is the retentate made up of nearly pure reactant A, but the flow rate of the retentate is also smaller when compared to the recycle stream in the distillation-only structures RD-D and RDWC-D (i.e., distillate of column C3).

Table 7
High chemical equilibrium — Costing information for the reactive distillation (RD) and its reactive dividing wall column (RDWC)/hybrid reactive dividing wall column (HRDWC) counterparts with conventional distillation column (D) and distillation-pervaporation (DP). Note that the dividing wall structures have the wall extended to the bottom of the main column.

Item	RD-D	RDWC-D	RD-DP	HRDWC-DP	Units
Capital cost (CAPEX)					
Column	4.3557	4.0634	3.7410	3.7398	M $
Membrane	–	–	0.5591	0.4605	M $
Reboiler	0.8030	0.8025	0.7778	0.7689	M $
Condenser	0.6425	0.5206	0.6294	0.5040	M $
Others	–	–	0.7385	0.7391	M $
Operating cost (OPEX)					
Waste	0.2528	0.2772	0.2038	0.1832	M $ y^{-1}
Heating	0.6732	0.6751	0.6141	0.5977	M $ y^{-1}
Cooling	0.0174	0.0174	0.0258	0.0272	M $ y^{-1}
Electricity	–	–	Trace	Trace	M $ y^{-1}
Mem. Rep.	–	–	0.0156	0.0129	M $ y^{-1}
Product (Component C, constraint = 99 mol%)					
Flow rate	11.34	11.18	11.56	11.68	kmol h^{-1}
Overall					
CAPEX	5.8013	5.3866	6.4459	6.2122	M $
Ann. CAPEX	0.7252	0.6733	0.8057	0.7765	M $ y^{-1}
OPEX	0.9434	0.9698	0.8594	0.8211	M $ y^{-1}
TAC	1.6686	1.6431	1.6651	1.5977	M $ y^{-1}
Prod. TAC	0.2002	0.1999	0.1956	0.1858	M $ kg^{-1}

Unlike in the low chemical equilibrium case, where the membrane cost took up about 13% of the CAPEX, in the high chemical equilibrium case, as shown in Figure S3.2, the membrane takes up only about 4% of the CAPEX. This is because when the chemical equilibrium is high, the conversion is higher, leading to a smaller amount of azeotrope and thus less membrane is required. Also, the cost of other equipment (auxiliary equipment for the membrane system, such as coolers, heaters, and pumps) is larger than the cost of the membrane itself. This is because there is a head cost to all the auxiliary equipment, and the head cost is independent of the number of membranes used. Therefore, when only a small number of membranes is required, the costs of the auxiliary equipment will relatively speaking exceed the cost of the membranes. Looking at the reboiler and condenser costs in all the designs, it can be seen that the condenser and reboiler costs are similar because, as shown in Table 6, the heating and cooling duties are similar.

Considering the OPEX, Fig. 7 shows that the overall operating cost for the hybrid structures is slightly lower than that of the standard structures, with up to 14% energy saving. Moreover, the heating cost and waste treatment are the first and second most significant contributions to the OPEX for all structures. Starting with the waste treatment, the hybrid structures require a much smaller cost (up to 34% reduction) due to the larger flow rate of the product C stream, leading to a lower amount of waste stream. As discussed earlier, for the hybrid structures, the distillate stream from column C3 (mainly azeotrope AC) is further processed in the membrane system, and only pure reactant A is recycled back to the reactive zone, which will improve the reaction and separation efficiency, resulting in a higher product C flow rate. For the heating cost, since all units use the same heating utility (recall that the utility type is automated during simulation and optimisation), the heating cost is directly proportional to the heating duty. It is therefore not surprising that the hybrid structure requires

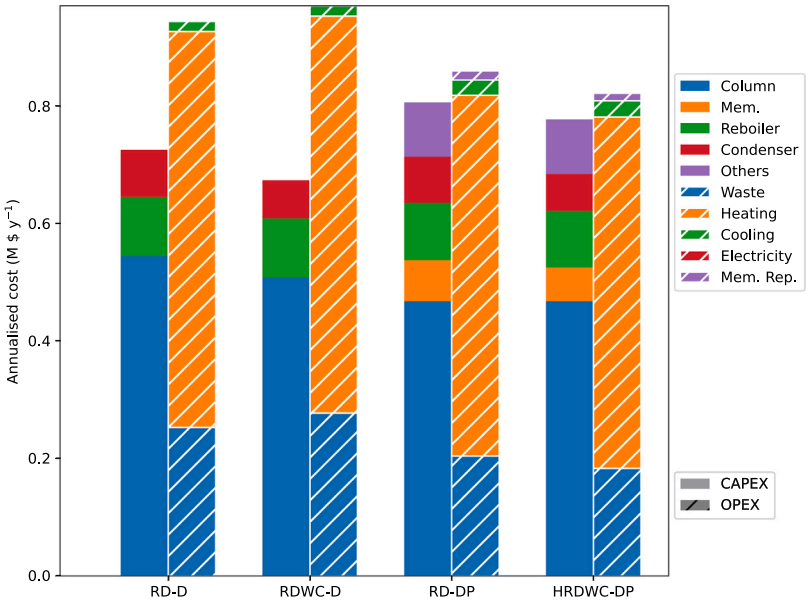

Fig. 7. High chemical equilibrium — Stacked bar graph showing the breakdowns of the annualised capital cost (CAPEX) and operating cost (OEPX) for reactive distillation-distillation (RD-D), reactive dividing wall column-distillation (RDWC-D), reactive distillation-distillation-pervaporation (RD-DP), and hybrid reactive dividing wall column-distillation-pervaporation (HRDWC-DP). Note that the dividing wall structures have the wall extended to the bottom of the main column.

less operating cost similar to the findings for low chemical equilibrium. For the cooling utility, as explained before, the permeate cooling uses expensive refrigerant (−50 °C). Although the hybrid structures' total cooling duty is lower, the cooling cost is higher. However, the cooling duty for permeate cooling is significantly lower than for other units, and therefore does not affect the overall operating cost much. The hybrid structures require additional costs for electricity (used in the pump) and membrane replacement. Due to the relatively small size of the membrane network, the membrane replacement cost is small for the membrane considered in this work.

Overall, the hybrid structures have lower production-based TAC, with about 7% reduction between HRDWC-DP and RD-D. It should be noted that the RD-DP structure has higher TAC than the RDWC-D structure. However, the final production-based TAC is lower due to the higher product flow rate in RD-DP.

4.3. Overall comparison

An overall comparison between the designs for both low and high chemical equilibrium shows that the base structures of RD-PS or RD-D and the DP designs, and their respective DWC equivalents, have similar distillation column structures (e.g., total number of stages, feed locations, side stream locations), indicating that the base and hybrid structures can be retrofitted into one another simply by reconnecting the distillate stream of column C3 either to another conventional distillation column or to a membrane network.

Considering the energy consumption in both cases, the dividing wall structure does not guarantee energy saving. From the optimisation results for the dividing wall structures, the heavy reactant B (which is the component with the highest boiling point) also leaves the prefractionator from the top thermal coupling stream because its feed stage is close to the top of the column, which interrupts the composition development in the main column.

It is also found that the hybrid structures always have a much higher CAPEX due to the expensive membrane system but with a reduced OPEX, meaning that the hybrid structure can always achieve energy savings compared to the base designs for the membrane considered in this work. Therefore, using the hybrid structure is a tradeoff between high CAPEX and low OPEX. For the cases investigated, the hybrid structures are preferred (lower production-base TAC) for high chemical equilibrium when the amount of permeate is smaller. This finding is also supported by a previous study [13] which compared the hybrid process with extractive distillation for a binary azeotropic mixture (ethanol-water system) with changing feed composition of ethanol. In that study, the hybrid process was only economically beneficial when the feed composition of ethanol was lower than 0.3 mol mol^{-1}, where ethanol is the component permeating through the membrane system. It should be noted that the membrane system requires extra equipment, such as pumps, heaters, and coolers, to achieve the separation. For a small size of membrane structures (i.e., for the high chemical equilibrium case), the cost of the extra equipment is comparable to the cost of membranes for the membrane system considered.

A comparison between low and high chemical equilibrium cases shows that the reduction in production-based TAC for high chemical equilibrium is due to the saving in OPEX (e.g., RD-DP saves 34.6% OPEX). Moreover, in both cases, the OPEX (mainly heating) is the most significant contribution to the overall cost for each structure. These two findings indicate that using a better catalyst and performing a heat integration can potentially improve the performances of the structures. The hybrid process could be further improved using a membrane with larger selectivity or lower cost. Furthermore, in this work, the expensive refrigerant is used for the membrane system to condense the permeate vapour due to a low permeate pressure (400 Pa) applied. Considering the permeate and retentate pressures as optimisation variables may avoid using refrigerant, which could further reduce the cost of the hybrid process.

It is worth noting that PS design and hybrid distillation-membrane process are both limited to specific conditions. For example, PS design can be used only for pressure-sensitive azeotropic systems. Considering the hybrid process, the lack of a suitable membrane for a specific mixture often limits the industrial applications of the hybrid process. If neither PS design nor the hybrid process can be used, extractive distillation or azeotropic distillation could also be considered by introducing an entrainer. The methodology followed in this work for the investigation can then follow along similar lines.

4.4. Discussions

Recall that the two main aims of this work are to (1) study the effect of chemical equilibrium (low and high) on possible column designs,

and (2) validate the technical and economic feasibility of HRDWCs. To achieve the first aim, artificial components are more efficient as the component property and reaction kinetics can be manipulated to suit the research needs. If a real mixture is considered, it is challenging to find two suitable catalysts for low and high chemical equilibrium, which is required for the research in this work. Also, it is important to start from a relatively simple system (e.g., A + B ⇌ C + D with one binary azeotrope) for proof-of-concept before moving on to a more complex, real-world system (e.g., esterification process with multiple azeotropes). This is because a complicated system is more likely to exhibit complex interactions/phenomena (than simpler systems), which may mask some basic findings that would otherwise be obvious when using simple systems. Therefore, since this study on HRDWC (recall that only a few studies in open literature have considered HRDWC) is in the proof-of-concept stage, it is more suitable to use a simple system so that most, if not all, basic interactions/phenomena can be observed clearly. Moreover, a more complex system calls for a more specific structure, while the structures generated for a simple system can be modular and thus can be easily modified to fit different systems. For example, if one requires a structure for A + B ⇌ C with A and C forming a minimum boiling azeotrope, the proposed structure can also be applied by simply removing column C2. Even for real esterification problems where there are more azeotropes, the concepts of generating the HRDWC (refer to Section 2.2.1) for this simple case can still be applied; instead of feeding the distillate of column C1 to an azeotropic separation sequence (e.g., PS distillation or membranes), the distillate can be fed to another distillation column to separate the different azeotropes further before sending them to the azeotropic separation sequence.

In terms of membrane systems, it should be noted that, for real-world examples, the membrane performance may be better or worse compared with the membrane utilised in this work as they may have different parameters (e.g., maximum allowable temperature, permeate and/or retentate pressure). However, the performance deviation, provided that the membrane selectivity does not deviate significantly, will only lead to a smaller or larger membrane network but not affect the overall structure. For example, in [13], using membranes with a higher maximum allowable temperature reduced the membrane network size (i.e., smaller total membrane area required), but the overall structure remains the same. Moreover, from the design comparisons, it was found that the conventional structures can easily be retrofitted into the hybrid structures because their RD column (column C1 for non-reactive dividing wall column and columns C1 + C3 for reactive dividing wall columns) are similar (i.e., RD-PS/RDWC-PS can be retrofitted into RD-DP/HRDWC-DP by replacing the PS columns with a membrane network without changing the RD column), thereby retrofit their existing conventional design into the greener (i.e., less energy required) hybrid counterpart.

5. Conclusion

This work considered the separation of a quaternary reactive system (A + B ⇌ C + D) having a binary azeotrope between one of the reactants and one of the products (i.e., components A and C) for either low or high chemical equilibrium. We explored various process-intensified structures of reactive distillation (RD) columns, including reactive distillation with pressure swing (RD-PS), reactive distillation with a hybrid distillation-pervaporation process (RD-DP), reactive distillation with conventional distillation column (RD-D), and the integration of two of the columns in those structures to form a reactive dividing wall column system (RDWC-PS or HRDWC-DP).

For the case of low chemical equilibrium, the reactive dividing wall structures with the wall either in the middle (RDWC-PS-Mid and HRDWC-DP-Mid), or extended to the bottom (RDWC-PS-Bot and HRDWC-DP-Bot), were explored. The features of each structure in terms of design, energy consumption and cost were considered. It was shown that by considering DP structures, an energy saving of up to 24% in the total duty required can be achieved. Moreover, the hybrid structure is preferred for high chemical equilibrium where higher conversion of the reactants leads to a smaller amount of azeotropes produced, thus less membrane area required for separating the azeotrope.

From an industrial perspective, the results also showed that the conventional RD-PS can easily be retrofitted into an RD-DP as their column designs are very similar. Lastly, for both low and high chemical equilibrium, all dividing wall structures (HRDWC-PS/DP/etc.) demand lower production-base total annualised cost (TAC) when compared to their base counterparts.

The involvement of the reaction system and formation of azeotropes added many opportunities to form various highly process-intensified structures. Therefore, the structures proposed in this work should not be considered the universal solution for the separation of all reactive systems. A change in the separation mixture and its properties (e.g., boiling point order, number of azeotropes formed, relative volatility between components) will require the current structures to be re-evaluated. Considering all the different structures in a single model would make the problem a superstructure optimisation problem, which is not the scope of this work. Nevertheless, the general design concepts and techno-economical analysis outlined in this work can serve as a starting point for the design of hybrid reactive dividing wall columns.

In terms of further work, the controllability of these structures should be studied to evaluate the overall dynamic performance. Also of interest would be an investigation of the impact of the membrane performance as well as consideration of different or multiple azeotropes within the system.

CRediT authorship contribution statement

Fanyi Duanmu: Writing – original draft, Visualization, Validation, Software, Resources, Methodology, Investigation, Formal analysis, Data curation, Conceptualization. **Dian Ning Chia:** Writing – original draft, Visualization, Validation, Software, Resources, Methodology, Investigation, Formal analysis, Data curation, Conceptualization. **Aikaterini Tsatse:** Writing – review & editing, Methodology, Conceptualization. **Eva Sorensen:** Writing – review & editing, Supervision, Project administration, Funding acquisition.

Declaration of competing interest

The authors declare that they have no known competing financial interests or personal relationships that could have appeared to influence the work reported in this paper.

Data availability

Data will be made available on request.

Appendix A. Supplementary data

Supplementary material related to this article can be found online at https://doi.org/10.1016/j.cep.2024.109832.

References

[1] W.L. Luyben, Comparison of extractive distillation and pressure-swing distillation for acetone-methanol separation, Ind. Eng. Chem. Res. 47 (8) (2008) 2696–2707, http://dx.doi.org/10.1021/ie701695u.
[2] A.A. Kiss, Distillation technology - still Young and full of breakthrough opportunities, J. Chem. Technol. Biotechnol. 89 (4) (2014) 479–498, http://dx.doi.org/10.1002/jctb.4262, arXiv:1011.1669v3.
[3] M. Skiborowski, A. Harwardt, W. Marquardt, Conceptual design of distillation-based hybrid separation processes, Annu. Rev. Chem. Biomol. Eng. 4 (1) (2013) 45–68, http://dx.doi.org/10.1146/annurev-chembioeng-061010-114129.
[4] F. Lipnizki, R.W. Field, P.-K. Ten, Pervaporation-based hybrid process: A review of process design, applications and economics, J. Membr. Sci. 153 (2) (1999) 183–210, http://dx.doi.org/10.1016/S0376-7388(98)00253-1.

[5] V. Van Hoof, L. Van den Abeele, A. Buekenhoudt, C. Dotremont, R. Leysen, Economic comparison between azeotropic distillation and different hybrid systems combining distillation with pervaporation for the dehydration of isopropanol, Sep. Purif. Technol. 37 (1) (2004) 33–49, http://dx.doi.org/10.1016/j.seppur.2003.08.003.
[6] A. Tgarguifa, S. Abderafi, T. Bounahmidi, Energy efficiency improvement of a bioethanol distillery, by replacing a rectifying column with a pervaporation unit, Renew. Energy 122 (2018) 239–250, http://dx.doi.org/10.1016/j.renene.2018.01.112.
[7] I. Dejanović, L. Matijašević, Z. Olujić, Dividing wall column—a breakthrough towards sustainable distilling, Chem. Eng. Process.: Process Intensif. 49 (6) (2010) 559–580, http://dx.doi.org/10.1016/j.cep.2010.04.001.
[8] T. Waltermann, M. Skiborowski, Conceptual design of highly integrated processes - optimization of dividing wall columns, Chem. Ing. Tech. 89 (5) (2017) 562–581, http://dx.doi.org/10.1002/cite.201600128.
[9] A. Tsatse, S. Oudenhoven, A. ten Kate, E. Sorensen, Optimal design and operation of reactive distillation systems based on a superstructure methodology, Chem. Eng. Res. Des. 170 (2021) 107–133, http://dx.doi.org/10.1016/j.cherd.2021.03.017.
[10] A. Tsatse, S. Oudenhoven, A. ten Kate, E. Sorensen, An investigation of the interactions between system characteristics and controllability for reactive distillation systems, Chem. Eng. Process. - Process Intens. 171 (2022) http://dx.doi.org/10.1016/j.cep.2021.108712.
[11] A. Tsatse, S. Oudenhoven, A. ten Kate, E. Sorensen, A framework to evaluate the impact of uncertainty on design and operation of reactive distillation systems, Chem. Eng. Sci. 251 (2022) http://dx.doi.org/10.1016/j.ces.2022.117485.
[12] D.N. Chia, F. Duanmu, E. Sorensen, Single- and multi-objective optimisation of hybrid distillation-pervaporation and dividing wall column structures, Chem. Eng. Res. Des. 194 (2023) 280–305, http://dx.doi.org/10.1016/j.cherd.2023.04.041.
[13] D.N. Chia, E. Sorensen, Optimal design of hybrid distillation-membrane processes based on a superstructure approach, Chem. Eng. Res. Des. 194 (2023) 256–279, http://dx.doi.org/10.1016/j.cherd.2023.04.014.
[14] F. Duanmu, E. Sorensen, Optimal design of heat integrated reduced vapor transfer dividing wall columns, in: Computer Aided Chemical Engineering, Vol. 49, Elsevier, 2022, pp. 75–180, http://dx.doi.org/10.1016/B978-0-323-85159-6.50029-4.
[15] F. Duanmu, E. Sorensen, An optimization-based comparison of different dividing wall column configurations, in: 12th International Conference on Distillation & Absorption, Toulouse, France, 2022.
[16] J. Holtbruegge, H. Kuhlmann, P. Lutze, Process analysis and economic optimization of intensified process alternatives for simultaneous industrial scale production of dimethyl carbonate and propylene glycol, Chem. Eng. Res. Des. 93 (May) (2015) 411–431, http://dx.doi.org/10.1016/j.cherd.2014.05.002.
[17] C. Wang, C. Wang, C. Guang, J. Gao, Z. Zhang, Hybrid reactive distillation using polyoctylmethylsiloxane membrane for isopentyl acetate production from mixed PVA by products, J. Chem. Technol. Biotechnol. 94 (2) (2019) 527–537, http://dx.doi.org/10.1002/jctb.5799.
[18] J. Li, T. Wang, Coupling reaction and azeotropic distillation for the synthesis of glycerol carbonate from glycerol and dimethyl carbonate, Chem. Eng. Process.: Process Intensif. 49 (5) (2010) 530–535, http://dx.doi.org/10.1016/j.cep.2010.04.003.
[19] W. Li, R. Sreerangappa, J. Estager, J.-C.M. Monbaliu, D.P. Debecker, P. Luis, Application of pervaporation in the bio-production of glycerol carbonate, Chem. Eng. Process. - Process Intensif. 132 (2018) 127–136, http://dx.doi.org/10.1016/j.cep.2018.08.014.
[20] P.U. Okoye, A. Longoria, P.J. Sebastian, S. Wang, S. Li, B.H. Hameed, A review on recent trends in reactor systems and azeotrope separation strategies for catalytic conversion of biodiesel-derived glycerol, Sci. Total Environ. 719 (2020) 134595, http://dx.doi.org/10.1016/j.scitotenv.2019.134595.
[21] C. Noeres, E.Y. Kenig, A. Górak, Modelling of reactive separation processes: Reactive absorption and reactive distillation, Chem. Eng. Process.: Process Intensif. 42 (3) (2003) 157–178, http://dx.doi.org/10.1016/S0255-2701(02)00086-7.
[22] K. Huang, Q. Lin, H. Shao, C. Wang, S. Wang, A fundamental principle and systematic procedures for process intensification in reactive distillation columns, Chem. Eng. Process.: Process Intensif. 49 (3) (2010) 294–311, http://dx.doi.org/10.1016/j.cep.2010.02.008.
[23] M.F. Malone, R.S. Huss, M.F. Doherty, Green chemical engineering aspects of reactive distillation, Environ. Sci. Technol. 37 (23) (2003) 5325–5329, http://dx.doi.org/10.1021/es034467w.
[24] G.J. Harmsen, Reactive distillation: the front-runner of industrial process intensification: A full review of commercial applications, research, scale-up, design and operation, Chem. Eng. Process.: Process Intensif. 46 (9) (2007) 774–780, http://dx.doi.org/10.1016/j.cep.2007.06.005.
[25] A. Gorak, Z. Olujic, Distillation: Equipment and Processes, Elsevier Academic Press, London, 2014.
[26] J. Marriott, E. Sorensen, The optimal design of membrane systems, Chem. Eng. Sci. 58 (22) (2003) 4991–5004, http://dx.doi.org/10.1016/j.ces.2003.07.011.
[27] Process Systems Enterprise, gPROMS process version 2.2, 2021.
[28] M. Tsuyumoto, K. Akita, A. Teramoto, Pervaporative transport of aqueous ethanol: dependence of permeation rates on ethanol concentration and permeate side pressures, Desalination 103 (3) (1995) 211–222, http://dx.doi.org/10.1016/0011-9164(95)00074-7.
[29] Process Systems Enterprise, Go:run, 2022.
[30] T. Bäck, D.B. Fogel, Z. Michalewicz (Eds.), Evolutionary Computation, Institute of Physics Publishing, Bristol ; Philadelphia, 2000.
[31] A. Umbarkar, P. Sheth, Crossover operators in genetic algorithms: a review, ICTACT J. Soft Comput. 06 (01) (2015) 1083–1092, http://dx.doi.org/10.21917/ijsc.2015.0150.
[32] A.P. Engelbrecht, Computational Intelligence: An Introduction, second ed., John Wiley & Sons, Chichester, England ; Hoboken, NJ, 2007.
[33] A.H. Gandomi, A.R. Kashani, Probabilistic evolutionary bound constraint handling for particle swarm optimization, Oper. Res. 18 (3) (2018) 801–823, http://dx.doi.org/10.1007/s12351-018-0401-6.
[34] K. Deb, An efficient constraint handling method for genetic algorithms, Comput. Methods Appl. Mech. Engrg. 186 (2–4) (2000) 311–338, http://dx.doi.org/10.1016/S0045-7825(99)00389-8.
[35] S. Melles, J. Grievink, S.M. Schrans, Optimisation of the conceptual design of reactive distillation columns, Chem. Eng. Sci. 55 (11) (2000) 2089–2097, http://dx.doi.org/10.1016/S0009-2509(99)00497-2.
[36] K. Sundmacher, Z. Qi, Conceptual design aspects of reactive distillation processes for ideal binary mixtures, Chem. Eng. Process.: Process Intensif. 42 (3) (2003) 191–200, http://dx.doi.org/10.1016/S0255-2701(02)00088-0.
[37] M. Al-Arfaj, W.L. Luyben, Comparison of alternative control structures for an ideal two-product reactive distillation column, Ind. Eng. Chem. Res. 39 (9) (2000) 3298–3307, http://dx.doi.org/10.1021/ie990886j.
[38] W.L. Luyben, Economic and dynamic impact of the use of excess reactant in reactive distillation systems, Ind. Eng. Chem. Res. 39 (8) (2000) 2935–2946, http://dx.doi.org/10.1021/ie000004c.
[39] D.B. Kaymak, W.L. Luyben, Quantitative comparison of reactive distillation with conventional multiunit reactor/column/recycle systems for different chemical equilibrium constants, Ind. Eng. Chem. Res. 43 (10) (2004) 2493–2507, http://dx.doi.org/10.1021/ie030832g.
[40] Y.-C. Cheng, C.-C. Yu, Effects of feed tray locations to the design of reactive distillation and its implication to control, Chem. Eng. Sci. 60 (17) (2005) 4661–4677, http://dx.doi.org/10.1016/j.ces.2005.03.033.
[41] R. Agrawal, Thermally coupled distillation with reduced number of intercolumn vapor transfers, AIChE J. 46 (11) (2000) 2198–2210, http://dx.doi.org/10.1002/aic.690461112.
[42] R. Agrawal, Synthesis of multicomponent distillation column configurations, AIChE J. 49 (2) (2003) 379–401, http://dx.doi.org/10.1002/aic.690490210.
[43] KBC Advanced Technologies, Multiflash version 6.1, 2015.
[44] S. Steinigeweg, J. Gmehling, Esterification of a fatty acid by reactive distillation, Ind. Eng. Chem. Res. 42 (15) (2003) 3612–3619, http://dx.doi.org/10.1021/ie020925i.
[45] M. Tsuyumoto, A. Teramoto, P. Meares, Dehydration of ethanol on a pilot-plant scale, using a new type of hollow-fiber membrane, J. Membr. Sci. 133 (1) (1997) 83–94, http://dx.doi.org/10.1016/S0376-7388(97)00090-2.
[46] J. Bausa, W. Marquardt, Shortcut design methods for hybrid membrane/distillation processes for the separation of nonideal multicomponent mixtures, Ind. Eng. Chem. Res. 39 (6) (2000) 1658–1672, http://dx.doi.org/10.1021/ie990703t.
[47] W.L. Luyben, Control of a column/pervaporation process for separating the ethanol/water azeotrope, Ind. Eng. Chem. Res. 48 (7) (2009) 3484–3495, http://dx.doi.org/10.1021/ie801428s.
[48] R.M. Dragomir, Synthesis and Design of Reactive Distillation Columns (Ph.D. thesis), University of Manchester, Manchester, 2004.
[49] F. Duanmu, D.N. Chia, E. Sorensen, A shortcut design method for complex distillation structures, Chem. Eng. Res. Des. 180 (2022) 346–368, http://dx.doi.org/10.1016/j.cherd.2022.02.026.
[50] B. Kaibel, Chapter 5 - dividing-wall columns, in: A. Górak, Z. Olujić (Eds.), Distillation: Equipment and Processes, Academic Press, Boston, 2014, pp. 183–199, http://dx.doi.org/10.1016/B978-0-12-386878-7.00005-X.
[51] R. Muthia, A.G.J. van der Ham, M. Jobson, A.A. Kiss, Effect of boiling point rankings and feed locations on the applicability of reactive distillation to quaternary systems, Chem. Eng. Res. Des. 145 (2019) 184–193, http://dx.doi.org/10.1016/j.cherd.2019.03.014.